Mitochondrial genomes and thousands of ultraconserved elements resolve the taxonomy and historical biogeography of the Euphonia and Chlorophonia finches (Passeriformes: Fringillidae)

Authors: Imfeld, Tyler S., Barker, F. Keith, and Brumfield, Robb T.

Source: The Auk, 137(3) : 1-25

Published By: American Ornithological Society

URL: https://doi.org/10.1093/auk/ukaa016

The Auk
Ornithological Advances

AmericanOrnithology.org

Volume 137, 2020, pp. 1–25
DOI: 10.1093/auk/ukaa016

RESEARCH ARTICLE

Mitochondrial genomes and thousands of ultraconserved elements resolve the taxonomy and historical biogeography of the *Euphonia* and *Chlorophonia* finches (Passeriformes: Fringillidae)

Tyler S. Imfeld,[1,2,*] F. Keith Barker,[1,2] and Robb T. Brumfield[3,4]

[1]Department of Ecology, Evolution, and Behavior, University of Minnesota, St. Paul, Minnesota, USA
[2]Bell Museum, University of Minnesota, St. Paul, Minnesota, USA
[3]Department of Biological Sciences, Louisiana State University, Baton Rouge, Louisiana, USA
[4]Museum of Natural Science, Louisiana State University, Baton Rouge, Louisiana, USA
*Corresponding author: imfel001@umn.edu

Submission Date: November 20, 2019; Editorial Acceptance Date: March 5, 2020; Published April 16, 2020

ABSTRACT

Relationships of the Neotropical finches in the genera *Euphonia* and *Chlorophonia* (Fringillidae: Euphoniinae) have been clarified by recent molecular studies, but species-level relationships within this group have not been thoroughly addressed. In this study, we sampled specimens representing every recognized species of these genera, in addition to 2 outgroup taxa, and used target enrichment to sequence thousands of ultraconserved element (UCE) loci, as well as mitochondrial DNA reconstructed from off-target reads, from each specimen to infer these relationships. We constructed both concatenation and coalescent-based estimates of phylogeny from this dataset using matrices of varying levels of completeness, and we generated a time-scaled ultrametric tree using a recently published fossil-based external calibration. We found uniformly strong support for a monophyletic subfamily Euphoniinae and genus *Chlorophonia*, but a paraphyletic *Euphonia* across UCEs and mitochondrial genomes. Otherwise, our inferred relationships were largely concordant with previous studies. Our time-tree indicated a stem divergence time of 13.8 million years ago for this lineage, followed by a relatively young crown age of only 7.1 myr. Reconstructions of biogeographic history based on this tree suggest a South American origin for crown Euphoniinae, possibly resulting from a transoceanic dispersal event from the Eastern Hemisphere, followed by 2 dispersal events into the Caribbean and as many as 6 invasions of North America coinciding with recent estimates of the age at which the Isthmus of Panama had completely formed. We recommend splitting *Euphonia* and resurrecting the genus *Cyanophonia* for the 3 blue-hooded species more closely related to *Chlorophonia*. Based on our results, we suspect that there is undescribed species-level diversity in at least one, possibly many, widespread and phenotypically diverse species.

Keywords: *Chlorophonia*, *Euphonia*, historical biogeography, mitochondrial genome, molecular systematics, ultraconserved elements

Los genomas mitocondriales y miles de elementos ultra-conservados resuelven la taxonomía y la historia biogeográfica de *Euphonia* y *Chlorophonia* (Paseriformes: Fringillidae)

RESUMEN

Las relaciones de los pinzones neotropicales en los géneros *Euphonia* y *Chlorophonia* (Fringillidae: Euphoniinae) han sido esclarecidas por estudios moleculares recientes, pero las relaciones a nivel de especie dentro de este grupo no han sido abordadas completamente. En este estudio, muestreamos especímenes que representan cada especie reconocida de estos géneros, además de dos taxones externos, y usamos enriquecimiento dirigido para secuenciar miles de loci de elementos ultra-conservados (EUC), así como ADN mitocondrial reconstruido a partir de lecturas fuera de rango, de cada uno de los especímenes, para inferir estas relaciones. Construimos estimaciones de filogenia tanto concatenadas como basadas en coalescencia a partir de esta base de datos usando matrices de niveles variables de integridad, y generamos un árbol ultra-métrico a escala temporal usando una calibración externa recientemente publicada basada en fósiles. Encontramos un fuerte apoyo para una subfamilia monofilética Euphoniinae y para el género *Chlorophonia*, pero un género parafilético de *Euphonia* a través de los EUCs y del genoma mitocondrial. De otra manera, las relaciones que inferimos fueron concordantes en gran medida con estudios previos. Nuestro árbol de tiempo indicó un tiempo de divergencia de una rama de 13.8 millones de años atrás para este linaje, seguido de una corona de edad relativamente joven de solo 7.1 millones de años. Las reconstrucciones de la historia biogeográfica basadas en este árbol sugieren un origen de América del Sur para la corona Euphoniinae, posiblemente como resultado de un evento de dispersión transoceánica desde el Hemisferio Oriental, seguido por dos eventos de dispersión en el Caribe y hasta seis invasiones

de América del Norte coincidiendo con estimaciones recientes de la edad a la cual se formó completamente el Istmo de Panamá. Recomendamos dividir *Euphonia* y reestructurar el género *Cyanophonia* para las tres especies con capucha azul más cercanamente emparentadas con *Chlorophonia*. Con base en estos resultados, sospechamos que hay una diversidad no descripta a nivel de especie en al menos una, posiblemente muchas, especies ampliamente distribuidas y fenotípicamente diversas.

Palabras clave: biogeografía histórica, *Chlorophonia*, elementos ultra-conservados, *Euphonia*, genoma mitocondrial, sistemática molecular

INTRODUCTION

The Neotropics are home to an abundance of endemic, highly distinct avian lineages and this is especially the case for passerine birds (Passeriformes). These lineages span substantial taxonomic breadth within the order, especially the remarkably species-rich suboscines (Tyranni), but a number of unique lineages of oscines (Passeri), such as the tanagers (Thraupidae; Burns et al. 2014), also evolved in the Neotropics. The 27 species in the genus *Euphonia* and 5 species in the genus *Chlorophonia* compose an endemic subfamily of the Fringillidae whose affinities were, frankly, long misunderstood. When compared with other species in their family, these birds emerge as unique, highly specialized organisms that have undergone a substantially different evolutionary trajectory from the remainder of species in their family. This group is essentially Neotropical in its distribution, with species ranging as far north as southern Sonora, Mexico (*Euphonia affinis*), and as far south as northern Argentina and eastern Paraguay (*Euphonia chlorotica*; Isler and Isler 1999, Chesser et al. 2018, Gill and Donsker 2019). All species are found in forested or woodland habitats of some kind, although individual species vary regarding whether they occupy edges or interiors and in which forest stratum they occur. Many species occupy low- and mid-level strata, but several others are specialists of forest canopies. Consequently, their natural history is relatively poorly known. Elevational ranges of euphonias and chlorophonias vary tremendously as well, with many species occurring in lowland areas down to sea level and others ranging up to the timberline in the Cordillera Talamanca (*Chlorophonia callophrys*) and over 3,000 m in the Andes (*Chlorophonia pyrrhophrys*). These species' reliance upon tropical forest ecosystems is likely due to their diet, which consists largely of fruit.

Euphonias and chlorophonias are often described as being dedicated mistletoe specialists that forage exclusively on these plants, but this is true for only a handful of species, such as *Euphonia elegantissima* (Reid 1991). Nearly all species are frugivorous at least in part during their annual cycles and take fruit from a diversity of plants, including *Ficus* spp., *Cecropia* spp., *Piper* spp., and melastomes. With few exceptions, species in this group have also been documented foraging for arthropods (Pérez-Rivera 1991). One of the striking aspects of the frugivorous habits of these birds is the degree of specialization in their gastrointestinal morphology. Euphonia gizzards are remarkably reduced, lacking any notable musculature or rigidity and resembling a continuation of the proventriculus extending to the small intestine (Forbes 1880, Wetmore 1914). This reduction of the gizzard appears to have convergently evolved in other passerines that are known to forage extensively on mistletoes, including flowerpeckers (Dicaeidae) of southern Asia and Australasia (Desselberger 1931) and silky-flycatchers (Ptiliogonatidae) of North America (Walsberg 1975), and appears to allow for rapid passage of fruits through the digestive tract. In the absence of mechanical processing by the gizzard, euphoniines have been observed processing fruit with their bills prior to ingestion as a form of mastication (Wetmore 1914, Isler and Isler 1999; T. S. Imfeld personal observation). These adaptations are notably divergent from typical true finches, which are omnivorous and generally forage on both insects and seeds throughout their annual cycles.

In addition to their Neotropical range, habitat preferences, and diet, the nesting behavior of euphoniines is quite different from many finches as well, in that they produce domed nests with side entrances constructed with grass, petioles, small twigs, and moss (Isler and Isler 1999). All of these traits, in addition to their colorful plumage, led to these birds' original classification as tanagers in the family Thraupidae, a group to which they are superficially much more similar. The only work to delve into relationships within *Euphonia* and *Chlorophonia* was Isler and Isler (first edition 1987), in which they recognized 4 species in *Chlorophonia*, 1 of which has since been split (*C. callophrys* split from *occipitalis*), and broke down the 25 then-recognized species in *Euphonia* (*E. elegantissima* and *cyanocephala* since split from *musica*) into 8 species groups based on shared plumage patterns, behaviors, and habitat preferences (pp. 223, table 20). Most *Euphonia* species were concretely classified into their respective groups based on these obvious shared traits, but several were either tentatively assigned to a group in the absence of clear relatedness to other species or groups. The disparate appearance, range, and behaviors of 2 relatively distinct species, *E. jamaica* and *minuta*, led Isler and Isler to classify them in their own monotypic species groups.

Such classification according to morphological and ecological similarity was the long-standing systematic standard by which families were described—species that

physically resembled each other and exhibited similar behaviors were traditionally grouped together. Examples of such traditional classification schemes include the Neotropical honeycreeper family Coerebidae (Hellmayr 1936), the flycatcher and thrush family Muscicapidae (Mayr and Amadon 1951), babblers (Hartert 1910), and even the family Fringillidae itself. However, with the advent and subsequent growth of molecular systematics beginning in the late 20th century, our understanding of phylogenetic relationships of many avian lineages has changed radically. With regard to the previous examples, Neotropical honeycreepers clearly fall within the tanager family Thraupidae but are polyphyletic (Burns et al. 2003), the traditional family Muscicapidae has been split into numerous families along with the reassigning of many genera (Cibois and Cracraft 2004, Voelker and Spellman 2004), family- and genus-level relationships within babblers have changed substantially (Cibois 2003, Reddy and Cracraft 2007, Zhang et al. 2007, Gelang et al. 2009), and the family Fringillidae has undergone a similar splitting and reassigning at several taxonomic levels (Yuri and Mindell 2002, Barker et al. 2013). The euphonias and chlorophonias are no exception and have also been reclassified and undergone significant taxonomic revision from their traditional placement in Thraupidae.

A molecular phylogeny inferred from mitochondrial cytochrome *b* (cytB) sequences from several tanager taxa, including *Euphonia laniirostris* and *Chlorophonia flavirostris*, revealed that *Euphonia* and *Chlorophonia* form a monophyletic lineage that is not closely related to Thraupidae (Burns 1997). Further work a few years later included additional sequences from a second mitochondrial locus (ND2) and concluded that this lineage (represented by *Euphonia finschi*) is nested within the family Fringillidae, among the true finches (Klicka et al. 2000), and a later expanded sequence sampling to include several mitochondrial loci of *C. flavirostris* and *E. laniirostris* and converged on the same result (Yuri and Mindell 2002). Following these studies, *Euphonia* and *Chlorophonia* are now recognized as the monophyletic subfamily Euphoniinae, which is sister to the large subfamily Carduelinae within the true finch family Fringillidae.

The next phylogenetic study to sample multiple species from these genera and explore relationships within this lineage was published 10 yr later by Zuccon et al. (2012) as part of a larger study to clarify generic relationships within Fringillidae. This study utilized a total of 5 loci, 2 mitochondrial and 3 nuclear, and included sequences from 10 total species from this lineage, 1 from *Chlorophonia* and 9 from *Euphonia*. The resulting phylogeny led to 2 noteworthy conclusions regarding this lineage: (1) after the divergence of chaffinches and Brambling in the subfamily Fringillinae, the sister relationship of the subfamilies Euphoniinae and Carduelinae is fully supported; and (2) *Chlorophonia cyanea* was found to be sister to *Euphonia musica*, thus rendering the genus *Euphonia* paraphyletic. The species-level relationships inferred within *Euphonia* were largely concordant with the Isler and Isler species-group classifications and concretely placed some species that were originally tentatively grouped (e.g., *finschi*, *laniirostris*, and *violacea*). No further study has yet inferred the phylogenetic relations among euphoniine species or resolved genus-level taxonomic conflict, despite huge advances in the depth and scale of molecular systematics and phylogenomics in the last decade.

In this study, we resolved the phylogeny of Euphoniinae using ultraconserved elements (UCEs; Faircloth et al. 2012), which have been similarly used to infer phylogenies at many taxonomic scales within birds (McCormack et al. 2013, Smith et al. 2014, Bryson et al. 2016, White et al. 2017, Musher and Cracraft 2018, Winker et al. 2018, Younger et al. 2018, Andersen et al. 2019, Jønsson et al. 2019, Oliveros et al. 2019). We obtained specimens representing all recognized species within the subfamily Euphoniinae and used standard methods to sequence and analyze thousands of UCE loci from each individual. Our study tackled 3 major aims using these phylogenomic data. First, we built upon the phylogenetic findings of previous studies by inferring the first phylogeny of this group with complete taxon sampling using both concatenation and coalescent-based methods in maximum-likelihood (ML) and Bayesian frameworks. Second, after inferring this phylogeny, we assessed the potential paraphyly of the genus *Euphonia* with regard to *Chlorophonia* and make recommendations of taxonomic revision. Lastly, we used a time-calibrated ultrametric phylogeny of the subfamily to model the historical biogeography and the tempo of evolution of this lineage within the Americas.

METHODS

Taxonomic Sampling

We obtained loans of frozen or ethanol-preserved tissue samples for 4 *Chlorophonia* species and for 24 of 27 *Euphonia* species currently recognized by most taxonomic authorities (Gill and Donsker 2019, Chesser et al. 2018, Remsen et al. 2018) from the following natural history collections in the United States: the Louisiana State University Museum of Natural Science (LSUMZ), the Field Museum of Natural History (FMNH), the Yale Peabody Museum (YPM), and the United States National Museum of Natural History (USNM). We obtained 2 samples for *E. xanthogaster* that represent allopatric and phenotypically disparate subspecies, *quitensis* and *ruficeps*, of this widespread South American species. For the 3 *Euphonia* species (*chalybea*, *concinna*, and *trinitatis*) and 1 *Chlorophonia* (*occipitalis*) species where fresh tissues were not available, we obtained toe pad subsamples from

study skin specimens in the following collections: FMNH, the Bell Museum at the University of Minnesota (MMNH), and the Museum of Vertebrate Zoology at the University of California, Berkeley. Additionally, we utilized tissues from *Coccothraustes verpertinus* and *Spinus tristis* from the MMNH collection, plus existing UCE phylogenomic sequence data for *Fringilla montifringilla* and *Emberiza citrinella* (Moyle et al. 2016, Oliveros et al. 2019), to include these taxa as outgroups spanning relationships within, and sister to, the family Fringillidae, respectively. A complete list of the museum specimens included in this study and their collection localities is shown in Table 1.

DNA Extraction and Illumina Sequencing

For all but 3 of the tissue specimens utilized in this study, we extracted total DNA from a tissue subsample using a DNeasy Blood & Tissue Kit (Qiagen, Valencia, California, USA) following the manufacturer's instructions. We extracted total DNA from the remaining 3 tissue specimens using a phenol-chloroform extraction and Phase Lock Gel following standard protocols from QuantaBio (Beverly, Massachusetts, USA). To extract DNA from the 3 toe pad subsamples, we washed the samples twice in 100% EtOH, soaked them in 100% EtOH for 15 min, and repeated this washing and soaking procedure for 70% EtOH and for ddH_2O, but with a 30-min soak in ddH_2O. We then followed a modified Qiagen DNeasy procedure. Specifically, we added an additional 20 µL of Proteinase K and 30 µL of dithiothreitol at 100 ng μL^{-1} concentration during the digestion, and these samples were incubated on a shaker at 56°C set to 30 rpm overnight. Afterwards, we eluted the samples twice in 50 µL of elution buffer instead of 200 µL, and these separate elutions were pooled and reduced by vacuum drying to a volume of 60 µL. We assessed the concentration of all DNA extracts using a QuBit dsDNA high-sensitivity assay and the quality and range of fragment sizes were assessed by running 2 µL of genomic DNA on a 1% Tris-borate EDTA agarose gel.

Target capture and dual indexing for each specimen, except for *C. occipitalis*, was performed by Arbor Biosciences (Ann Arbor, Michigan, USA) using the Tetrapod 5k 1.8 MYbaits probe kit (ultraconserved.org) to target ~5,000 UCE loci from each sample of genomic DNA (Faircloth et al. 2012). Assembly of individual baited libraries for each specimen, enrichment reactions for 7 pooled libraries (with 5 specimens each), and library equilibration, was also performed by Arbor Biosciences following their MYreads protocols. The resulting equilibrated library was sequenced in one half lane of an Illumina NextSeq 550 (San Diego, California, USA) run to obtain 150 base pairs (bp) paired-end reads at the University of Minnesota Genomics Center (St. Paul, Minnesota, USA). For *C. occipitalis*, we targeted and sequenced ~1 kb of cytb by polymerase chain reaction (PCR). We amplified this locus in 5 segments due to the degraded state of the DNA extracted from the toepad subsample for this specimen, and each reaction had a volume of 25 µL and otherwise followed the procedures described by Barker et al. (2008). After performing an additional round of PCR, they were sequenced at the University of Minnesota Genomics Center. Raw read data from this study were accessioned in the National Center for Biotechnology Information (NCBI) Short Read Archive (BioProject ID: PRJNA604822).

Contig Assembly and Sequence Alignment

The resulting Illumina reads were trimmed to remove adapters and low-quality bases using *illumiprocessor* 2.0.9 (Faircloth 2013). We then used *phyluce* 1.5 to assemble sequence contigs and for all remaining steps prior to constructing the actual phylogenies (Faircloth 2016). We performed 2 contig assemblies of our read data using both *Trinity* 2.1.1 and *SPAdes* 3.12.0 to compare assembly quality and assess efficiency in mitogenome assembly. These contigs were then screened against the Tetrapod 5K UCE probe set to identify and then extract contigs that mapped to UCE element loci. We extracted these loci from the FASTA data into an incomplete sequence matrix and aligned these sequences using *MAFFT* 7.407. Using scripts in R 3.5.1 (R Core Team 2013), we then quantified these data to determine the number of UCE-matching contigs per specimen, the distribution of sequence lengths from these loci, and the total number of bp to be included in subsequent analyses. This incomplete sequence matrix was pared down to obtain an additional complete sequence matrix that only included UCE loci sequenced for every specimen in the dataset.

ML Phylogeny Inference

We converted the incomplete sequence matrix to a concatenated PHYLIP file to perform concatenated ML inference of the phylogeny in RAxML 8.2.9 (Stamatakis 2014). These analyses were preceded by running a UCE-specific partitioning algorithm, sliding window site characteristics of entropy (SWSC-EN; Tagliacollo and Lanfear 2018). Given the distinct structure of UCE loci, in which the core sequence is strongly conserved between species and the flanking regions vary considerably, this algorithm divides a concatenated alignment of UCE loci by splitting the sequence of each locus into 3 partitions representing the core and 2 flanking regions, and then partitioning the alignment given this heterogeneity in sequence variation. We modified this method slightly for the complete UCE alignment by increasing the window size from 50 to 100 bp to increase the minimum potential size of partitions in the final analysis. The output of this method for both the incomplete and complete sequence matrices was then

TABLE 1. Taxonomic sampling of this study. Collection abbreviations follow the main text, with the addition of the University of Kansas Biodiversity Institute (KU). An asterisk (*) indicates the sample used was a toe pad instead of a tissue subsample. A caret (^) indicates a female specimen. A tilde (~) indicates that previously generated UCE sequence data were used from this specimen. Group # corresponds to the *Euphonia* species groups following Isler and Isler (1999)

Taxon	Specimen ID	Group #	Locality
Fringilla montifringilla	KU 4293~	-	CN–Heilongjiang
Chlorophonia cyanea	LSUMZ 27729	-	PE–Loreto
Chlorophonia pyrrhophrys	LSUMZ 32512^	-	PE–Cajamarca
Chlorophonia flavirostris	LSUMZ 30315	-	EC–Esmerelda
Chlorophonia occipitalis	MMNH 34765^ *	-	MX–Veracruz
Chlorophonia callophrys	LSUMZ 41634	-	PA–Chiriquí
Chlorophonia callophrys	LSUMZ 27273	-	CR–Cartago
Euphonia jamaica	FMNH 331118	1	JM–Cornwall
Euphonia plumbea	LSUMZ 25459	2	BR–Amazonas
Euphonia affinis	LSUMZ 27271	2	CR–Alajuela
Euphonia chlorotica	LSUMZ 46235	2	PE–San Martín
Euphonia luteicapilla	LSUMZ 28445	2	PA–Panamá
Euphonia trinitatis	FMNH 258456*	2	CO–Magdalena
Euphonia concinna	MVZ 120660*	2	CO–Cundinamarca
Euphonia saturata	LSUMZ 67617	2	PE–Tumbes
Euphonia finschi	USNM 626136	2	GY–Upper Takutu-Upper Essequibo
Euphonia violacea	LSUMZ 69401	3	TT–Tunapuna-Piarco
Euphonia laniirostris	LSUMZ 66278	3	PE–Tumbes
Euphonia hirundinacea	LSUMZ 60936	3	HN–Cortés
Euphonia chalybea	FMNH 344839*	3	BR–São Paulo
Euphonia musica	LSUMZ 11319	4	PR–NA
Euphonia elegantissima	LSUMZ 16040	4	CR–Heredia
Euphonia cyanocephala	LSUMZ 38380	4	BO–Santa Cruz
Euphonia fulvicrissa	LSUMZ 46614	5	PA–Darién
Euphonia chrysopasta	LSUMZ 80699	5	BR–Amazonas
Euphonia mesochrysa	LSUMZ 39089	5	BO–Cochabamba
Euphonia imitans	LSUMZ 71975	5	CR–Puntarenas
Euphonia gouldi	FMNH 393879	5	MX–Veracruz
Euphonia minuta	LSUMZ 42576	6	PE–Loreto
Euphonia anneae	LSUMZ 28370	7	PA–Chiriquí
Euphonia xanthogaster quitensis	LSUMZ 66429	7	PE–Tumbes
Euphonia xanthogaster ruficeps	LSUMZ 39186	7	BO–Cochabamba
Euphonia cayennensis	YPM 139433	8	SR–Sipaliwini
Euphonia pectoralis	FMNH 427269	8	BR–Alagoas
Euphonia rufiventris	LSUMZ 10566	8	PE–Ucayali
Coccothraustes vespertinus	MMNH 42435	-	US–Minnesota
Spinus tristis	MMNH 46324	-	US–Minnesota
Emberiza cintrinella	LSUMZ 12240~	-	SW–Uppland

used as input to optimize the partitioning scheme and assign models to the resulting partitions in *PartitionFinder2* (Lanfear et al. 2017). Optimizing the partitioning scheme for the incomplete sequence matrix computationally failed due to the sheer number of possible partitioning schemes, so we manually set a scheme that partitioned the total aligned sequence into flanking regions, cores, and unsplit UCE loci. We then ran RAxML using the manual partitioning scheme for the incomplete sequence matrix and the best-supported partitioning scheme for complete sequence matrix and bootstrapped both analyses 100 times with the "-f a" option.

We performed a ML coalescent-based analysis using the incomplete sequence matrix in 2 steps. First, we generated individual PHYLIP files for each UCE locus in the incomplete sequence matrix, removed any loci that contained sequences for fewer than 4 taxa, and inferred gene trees for every individual locus using RAxML. Second, we used these gene trees as input to estimate a species tree for these data using ASTRAL-III 5.6.3 (Zhang et al. 2018). The nodal support and quantification of gene tree-species tree discordance for this coalescent-based topology were assessed using several metrics, including the localized posterior probability (LPP) computed by ASTRAL. In

addition, we calculated internode certainty (IC) scores for each branch in the species tree as implemented in RAxML, which calculates the frequency of gene tree topologies that differ from that of the species tree with regard to individual branches and whether these different topologies occur with equal frequencies as expected in the absence of gene flow. IC scores near 1 indicate high concordance between the species tree and gene trees, scores near 0 indicate equal frequencies of discordance with the species tree among alternative gene tree topologies, and IC scores near −1 indicate strong discordance with the species tree and highly skewed representation among the conflicting gene trees (Salichos et al. 2014). Further, we calculated 2 node-specific concordance factors as implemented in *IQ-TREE* (1.7-beta9), gene concordance factors (gCF) and site concordance factors (sCF) (Nguyen et al. 2015, Minh et al. 2018). These values quantify the proportion of informative gene trees and sites in the aligned sequences for a given node in the species tree that are concordant with that node, with both values ranging from 0 (high discordance of gene trees and informative sites) to 1 (high concordance of gene trees and informative sites). Next, we also assessed support for this topology by bootstrapping the gene tree topologies. We generated 100 bootstrap replicates by sampling all the gene tree topologies with replacement and, for each replicate, inferred a species tree of those sampled gene trees using ASTRAL. We then utilized this distribution of 100 bootstrapped species trees as the distribution of "gene trees" to compare with the true species tree topology and to compute a set of bootstrap values using the "f -b" option in RAxML. Finally, to further test the robustness of the species tree topology obtained from the incomplete sequence, we performed ASTRAL analyses on the complete sequence matrix and a 50% complete sequence matrix (containing at least 19 taxa), and we calculated concordance factors and internode certainty values as nodal support for these species trees. We then visually compared the resulting topologies to assess any conflicting nodes.

Mitochondrial Phylogenomics

In addition to analysis of the UCE data, we assembled and analyzed complete or near-complete mitochondrial genomes for the taxa that were sampled by target enrichment. Off-target mitochondrial reads were assembled in 1 of 2 ways. First, *Trinity* and *SPAdes* assemblies were inspected for single large contigs of ~16 kb in length that were good candidate mitogenomes. A set of mitochondrial genes from a related passerine (*Spinus spinus*, GenBank accession NC015198) were mapped to these contigs in *Geneious* 10.2.4 (Biomatters, Auckland, New Zealand), and gene presence and length and open reading frames were confirmed. Where possible, these contigs were circularized and their coordinate systems reset to start at the first base of tRNA-Phe. For samples without single large contigs in their corresponding assembly, we used *Geneious* to map reads from those samples to 1 of 3 complete, high coverage euphoniine mitogenomes (*C. cyanea*, *Euphonia musica*, or *Euphonia finschi*) most closely related to that sample based on UCE results. Assemblies with <90% estimated mitogenome coverage were excluded from further analysis. The consensus of the remaining assemblies was extracted and examined as described above, and these mitogenomes were annotated and submitted to GenBank (accession IDs: MT063155–MT063184).

Assembled euphoniine and outgroup mitogenomes were aligned using *MUSCLE* 3.8.425. An additional outgroup (*Agelaius phoeniceus*, GenBank accession JX516062) was included in this analysis to facilitate mapping of 48 standardized character sets (RNA stem and loop, protein coding gene codon positions, etc.; see Powell et al. 2013) onto the alignment. Model fitting for this alignment was performed recognizing these character sets, using *PartitionFinder2*, allowing only the GTR and GTR+G models with proportional branch lengths, using greedy optimization with AIC_c as an optimality criterion (Yang 1994). The mitogenome data were analyzed under the best fit partitioning and models using RAxML 8.2.11, calculating 1,000 bootstrap replicates.

Inference of a Time-calibrated Tree

While we consider the species tree topology inferred by ASTRAL to be the best estimate for the entirety of the UCE sequence data, ASTRAL is unable to estimate terminal branch lengths and only estimates internal branch lengths in coalescent units, rather than in units of absolute time. Another issue to overcome was the fact that *C. occipitalis* was not included in this tree. To estimate ultrametric, time-scaled branch lengths and node ages across this topology and to include all species, we inferred a tree using the partitioned, concatenated alignment of the complete UCE sequence matrix and the cytb sequences as one additional partition in BEAST 2.5.2 (Bouckaert et al. 2014). We extracted a cytb sequence from each complete mitochondrial genome and aligned these sequences with that from *C. occipitalis* using *MUSCLE* 3.8.425. Prior to the BEAST2 analysis, we performed an additional RAxML analysis on this new partitioned concatenated alignment using the "-g" option, which establishes a fixed starting tree, the ASTRAL species tree in this case, and optimizes the location of previously unsampled tips on this topology. Doing so allowed us to place *C. occipitalis* on the species tree topology. The tree resulting from this analysis was made ultrametric using the *chronos* function in the R package *ape* (Paradis et al. 2004), and we then used this resulting ultrametric phylogeny as the starting tree constraint in the BEAST2 analysis. We constrained the tree search in BEAST2 such that it would optimize

branch lengths for this topology given the complete-partitioned sequence alignment with cytb and not change the topology. We calibrated the absolute age of this tree by assigning a log-normal prior to the root node using information from a recent UCE-based phylogenomic study of all families in the order Passeriformes using 13 fossil calibrations and overlapping sequence data for 2 species shared between that study and the present one, *Fringilla montifringilla* and *Emberiza citrinella* (Oliveros et al. 2019). This prior separates *Emberiza* from the family Fringillidae and was set to have a mean of 2.8365 and a standard deviation of 0.0745 to match the highest posterior density interval of the node age and uncertainty inferred from the family-level maximum-clade credibility (MCC) tree. We configured the run to have a strict clock model linked across all partitions with a uniform prior set with the default values, and we set identical HKY+G substitution models for each individual partition in the alignment with the default distributions set by BEAUti 2.5.2 (Hasegawa et al. 1985). We originally specified a birth-death tree model with gamma-distributed priors of $\alpha = 0.001$ and $\beta = 1{,}000$ for both the birth and death rate and ran this analysis for 50,000,000 generations on the CIPRES Science Gateway (Miller et al. 2010).

This analysis reached convergence for every parameter in the model with high effective sample sizes except for the prior and the posterior, both of which had low effective sample size (ESS) values of only 8, which is a symptom of the model prior not having enough time to thoroughly mix and sample the entirety of the possible parameter space. Therefore, we modified our control file for the analysis by changing the birth-death tree model to a Yule model with a default uniform prior and by increasing the run length to 100,000,000 generations. We sampled the trace of this analysis every 10,000 generations, and sampled trees every 100,000 generations to generate a final posterior sample of 10,000 observations and a posterior distribution of 1,000 trees. Lastly, we determined whether this analysis had achieved convergence after its completion by analyzing its log in Tracer 1.7 (Rambaut et al. 2018).

Biogeographic Reconstruction

We obtained a MCC tree from the posterior distribution of trees sampled by the BEAST2 run in TreeAnnotator 2.5.2, specifying a 10% burn-in and obtaining median node heights, to reconstruct the biogeographic history of this lineage. We scored the biogeographic range of each species on this MCC tree as presence or absence in the following 4 biogeographic regions: North America (Mexico south to Darién, Panama); South America (Darién, Panama south to Brazil, Paraguay, and Argentina; including Trinidad); the Caribbean (any island in the Greater or Lesser Antilles, excluding Trinidad); and the Eastern Hemisphere (Eurasia, given the scope of sampling in this study). Only 3 species' ranges included more than 1 of these biogeographic regions given this scoring strategy (*E. fulvicrissa*, *E. laniirostris*, and *E. minuta*), so they were assigned as present in 2 regions, North and South America.

We compared the fit of 3 likelihood-based models of biogeographic range evolution, DEC, DIVALIKE, and BAYAREALIKE, using the *BioGeoBEARS* package in R (Matzke 2013a, b). All 3 models optimize parameters for anagenetic rates of range expansion or contraction (*d* or *e*) along the branches of a phylogeny but differ in their parameterization of cladogenetic range changes through vicariant or sympatric events. The BAYAREALIKE model only parameterizes simple sympatric cladogenetic events with the *y* parameter, whereas both the DEC and DIVALIKE models account for both sympatric and vicariant range change events with the parameters *y* and *v*. These 2 are further differentiated in that the DEC model contains an additional parameter, *s*, which defines sympatric speciation in a subset of the lineage's total range, whereas the DIVALIKE model allows for both narrow-range and widespread vicariance events. Additionally, *BioGeoBEARS* can modify these 3 models by including an additional parameter, *j*, which models the probability of founder-event speciation, but recent work has debated whether the likelihood of such models is directly comparable with those of alternative models that lack this parameter, making assessments of model fit problematic (Ree and Sanmartín 2018). Therefore, we only report results from fitting the DEC, DIVALIKE, and BAYAREALIKE models without *j* to these biogeographic range data.

RESULTS

Sequencing and UCE Contig Assembly

Illumina sequencing of the equilibrated library with the 35 specimens in this study yielded 136,882,528 reads with an average read length of 302 bp, altogether yielding a total of 41.4 Gb of sequence data. This includes an average of 3,910,929 reads per specimen, although there was a notable range from the lowest to the highest number of reads for an individual (142,031 for *Chlorophonia pyrrhophrys* to 6,501,897 for *Euphonia cyanocephala*). Using the *Trinity* assembly algorithm to analyze these read data, we obtained an average of 4,289 contigs matching UCE loci from each specimen, although the number of UCE-matching contigs ranged from a minimum of 3,779 in *C. pyrrhophrys* to a maximum of 4,486 in *Euphonia musica*. A total of 4,956 unique UCE loci were recovered across all samples, and the mean and median sequence lengths of these UCE contigs were 928 and 989 bp, respectively. A complete matrix including only UCE loci with sequences from all 37 specimens included in the study contained only 150 loci; however, a 95% complete matrix contained 1,278 loci, a 90% complete matrix contained 2,870 loci, and the 50% complete matrix

contained 4,829 loci. The *SPAdes* assembly performed comparably well in the recovery of UCE-matching contigs. Screening the results of this assembly yielded an average of 4,307 UCE contigs per specimen, with the minimum and maximum ranging from 3,776 to 4,486 in *C. pyrrhophrys* and *E. musica*, respectively. The mean sequence length for these UCE-matching contigs was 786, but the *SPAdes* assembly also included many additional contigs that, when screened against existing avian mitochondrial genome sequences, were found to comprise most, if not all, of the mitochondrial genome. These mitochondrial genomes were successfully assembled for every tissue specimen and were retained for separate phylogenetic analyses as a complement to the analyses performed with the *Trinity*-assembled nuclear UCE sequence data. The number of reads and the number of UCE-matching contigs for each specimen in the separate *Trinity* and *SPAdes* assemblies is provided in Appendix Table 3.

Maximum Likelihood UCE Phylogenies

The concatenated incomplete sequence alignment of all 4,956 loci used to infer a phylogeny in RAxML was 4,746,327 bp in length and was split into 3 partitions defining the flanking regions, the core regions, and the UCE loci that were not split by SWSC-EN. The tree resulting from this analysis was, overall, strongly resolved as interpreted from bootstrap percentages and only 3 nodes received bootstrap values less than 100% (Figure 1A). These nodes involved the placement of *E. saturata* (91%), *E. chlorotica* (88%), and the separation of (*E. anneae, E. xanthogaster*) from (*E. mesochrysa,* [*E. cayennensis*, {*E. rufiventris*, *E. pectoralis*}]) (93%). The best-supported partitioning scheme for the concatenated alignment of the complete sequence matrix contained 119 partitions, and the total length of this 150-locus alignment was 159,894 bp in length. The RAxML phylogeny inferred with this complete, partitioned sequence alignment was also strongly resolved overall with only 7 nodes receiving <100% bootstrap support and this tree possessed only 2 topological differences from the incomplete phylogeny (Figure 1B). The incomplete topology inferred a sister relationship between 2 small clades of *Euphonia* species (*anneae, xanthogaster*) sister to (*mesochrysa*, [*cayennensis,* {*rufiventris, pectoralis*}]) to the exclusion of another small *Euphonia* clade containing (*imitans*, [*gouldi, fulvicrissa*]), whereas the complete topology inferred the (*anneae, xanthogaster*) clade being 1 node lower and sister to the other 2 clades. Neither arrangement of these clades had full bootstrap support in their respective trees, although both are >90%. The incomplete tree had *E. jamaica* as the most divergent branch in its respective clade, whereas *E. saturata* is the most divergent in the complete topology. Both of these placements have bootstrap support >90%. A notable feature of these phylogenies was that the 3 blue-hooded *Euphonia* species (*cyanocephala*, *elegantissima*, and *musica*) form a monophyletic group that is sister to the monophyletic *Chlorophonia*, a result that is consistent with previous results that found *E. musica* and *C. cyanea* as sister taxa (Zuccon et al. (2012)). This relationship was recovered in all subsequent phylogenetic analyses of both the nuclear UCE and mitochondrial genomic data and its taxonomic implications for these genera are discussed further below.

A total of 4,944 UCE gene trees containing >3 species were utilized to estimate the species tree for this lineage in ASTRAL. The topology of this species tree had maximum support values at all but 2 nodes as indicated by the LPP scores obtained via ASTRAL, with only the nodes defining the placement of *E. chlorotica* and *E. saturata* having scores less than 1 (Table 2; 0.98 and 0.76, respectively). There were no negative IC scores for any relationship in the species tree, but these scores did range from 0 to 0.643 and were generally low across the tree (median = 0.147). Both sets of concordance factors had fairly broad ranges as well, with gCF values ranging from 10.4 to 79.2 (median = 32.5) and sCF ranging from 20.8 to 96.3 (median = 58.95). gCF and sCF values were both positively correlated with IC values (Figure 2), with sCF values generally higher as expected given the relatively low levels of homoplasy in these slowly evolving loci. The support values from our manual bootstrapping were largely concordant with the LPP scores for the tree obtained directly from ASTRAL; the only 2 nodes in the entire topology with bootstrap scores less than 100% were those placing *E. chlorotica* (90%) and *E. saturata* (87%). Taken together, these metrics illustrate that the species tree inferred by ASTRAL does not have any hard, consistent conflict with any alternative topologies in the full distribution of gene trees, despite the variation in topologies that were inferred among individual gene trees.

This 4,944-locus species tree possessed 1 distinct relationship not found in either of the concatenated RAxML trees, with *C. pyrrhophrys* as the deepest split in the genus *Chlorophonia* with relatively high support (gCF = 34.2, sCF = 77.9, IC = 0.091, bootstrap = 100%) rather than being sister to *C. cyanea*. Interestingly, the species tree's placement of the 3 *Euphonia* clades mentioned above is concordant with that of the incomplete RAxML phylogeny, although the support values for this node are fairly low (gCF = 10.9, sCF = 35.0, IC = 0.0, bootstrap = 100%), and the placement of *E. jamaica* and *saturata* in this species tree also follows that of the incomplete RAxML phylogeny albeit with relatively low certainty in the placement of *saturata* as noted above.

The species tree generated from analyzing the 50% complete sequence matrix was topologically identical to the incomplete matrix topology and is not discussed further here, but the complete matrix species tree did possess

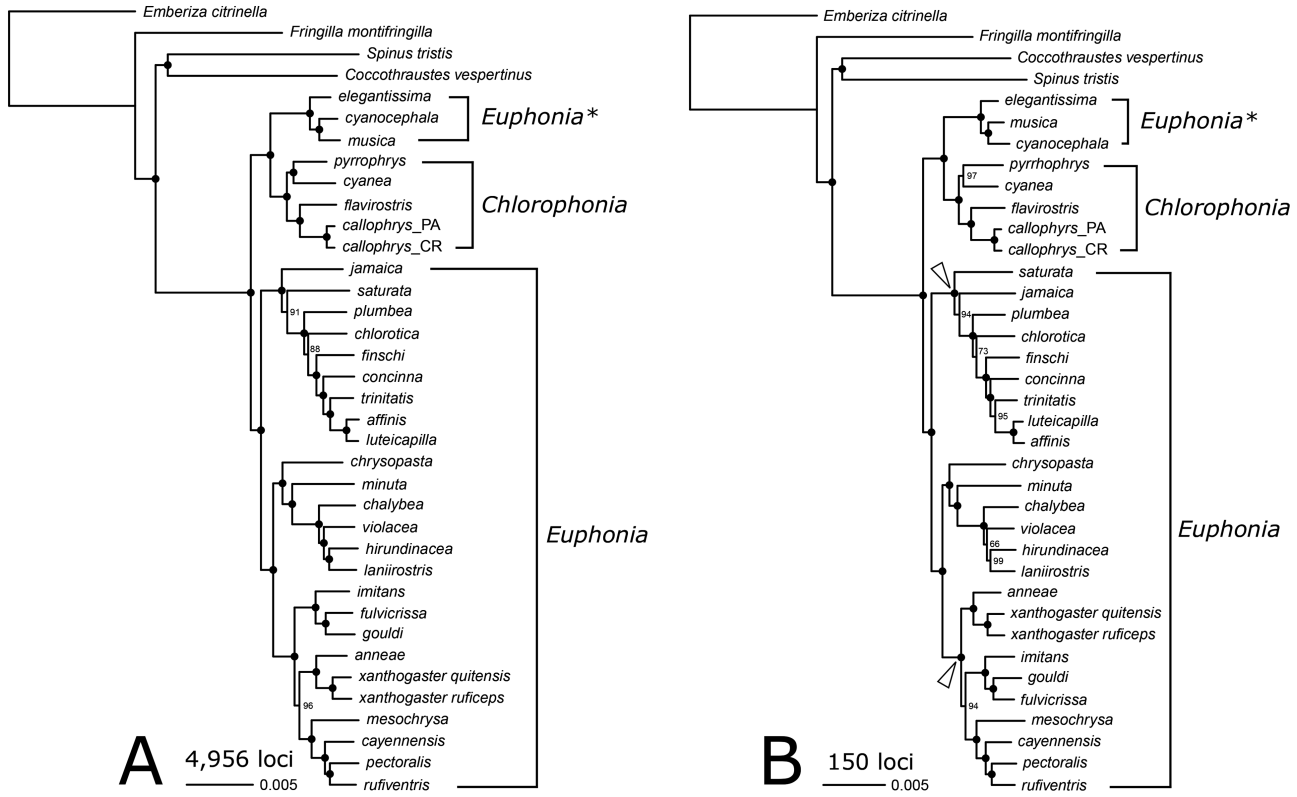

FIGURE 1. Concatenated phylogenies inferred from UCE sequences. The left tree (**A**) was generated from a partitioned analysis of 4,956 incompletely sampled loci and the right tree (**B**) from a partitioned analysis of 150 completely sampled loci. Black circles on nodes indicate 100% bootstrap support for that topology given its dataset and only nodes receiving <100% support have their bootstrap values reported on the tree. The white arrows point to the 2 topological differences between the trees: the arrangement of the 3 small *Euphonia* clades and of *E. jamaica* and *saturata*. The *Euphonia* clade marked with an asterisk designates the 3 blue-hooded species in this figure and in all following figures.

a few topological differences when compared with the incomplete matrix tree (Appendix Figure 5, Appendix Table 5). The order of *E. jamaica* and *E. saturata* flip, in that *jamaica* is sister to all other species within its clade in the incomplete matrix topology whereas *saturata* is sister to all others in this same clade in the complete matrix topology. A similar flip of branching order occurs with *E. concinna* and *E. finschi* in this same clade, with the incomplete matrix topology having *finschi* diverge before *concinna* and the opposite relationship being supported in the complete matrix topology. Lastly, the complete matrix topology yielded a unique ordering of the 3 small *Euphonia* clades described above in that the (*mesochrysa*, [*cayennensis*, {*rufiventris*, *pectoralis*}]) clade was sister to the other 2, and the root node of this arrangement was well supported (gCF = 32.7, sCF = 75.3, IC = 0.555), more so than the root node of these 3 clades in the incomplete matrix topology.

Mitochondrial Phylogeny

The phylogeny inferred from only the mitochondrial genome assemblies was largely concordant with our phylogenies inferred from the nuclear UCE loci, regardless of whether these loci were concatenated or analyzed with maximum likelihood or Bayesian methods (Figure 3). One sister species pair was inferred to have short branch lengths on this topology, with a total sequence divergence between *Euphonia affinis* and *luteicapilla* of 0.273%, and this shallow divergence was also reflected in the total UCE sequence alignment with 0.113% sequence divergence. Overall, the mitochondrial phylogeny was fairly well resolved, with all but 6 nodes receiving 100% bootstrap support. The other nodes lacking full support had bootstrap support ranging from 45 to 89%. Two points in this topology differed from either the concatenated phylogenies or the species tree. First, the relationship of the 3 small *Euphonia* clades matched that of the incomplete, concatenated phylogeny and the species tree with 100% bootstrap support, and only differs from the complete, concatenated phylogeny. Second, the mitochondrial data support a sister relationship of *C. pyrrhophrys* and *cyanea* with 100% bootstrap support, as is the case in the concatenated phylogenies with comparably high bootstrap support (97–100%). By contrast, the species tree reconstructed *pyrrhophrys* as the

TABLE 2. Node support values and node ages from the ASTRAL species tree topology of Euphoniinae. The full time-tree including the outgroups is provided in Appendix Figure 6 and the corresponding values for the nodes of those outgroups are provided in Appendix Table 4

Node	LPP	gCF	sCF	IC	Bootstrap	Age (Myr)	Age (95% HPD)
1	1	77.2	89.0	0.614	100	7.06	5.97–8.02
2	1	19.5	47.2	0.136	100	6.49	5.42–7.29
3	1	18.1	50.6	0.204	100	5.68	4.84–6.49
4	1	30.8	70.2	0.377	100	4.25	3.63–4.86
5	1	10.9	35.0	0.000	100	3.96	3.43–4.60
6	1	27.2	58.9	0.278	100	3.24	2.74–3.70
7	1	38.8	70.8	0.353	100	2.35	1.97–2.70
8	1	29.5	41.7	0.025	100	1.85	1.51–2.11
9	1	36.8	70.5	0.392	100	2.67	2.21–3.06
10	1	57.6	73.9	0.358	100	1.32	1.12–1.56
11	1	48.8	79.5	0.634	100	2.54	2.11–2.90
12	1	42.5	59.0	0.114	100	1.89	1.57–2.17
13	1	18.5	47.7	0.093	100	5.17	4.35–5.85
14	1	23.7	50.0	0.116	100	4.58	3.88–5.24
15	1	52.6	86.4	0.510	100	2.58	2.18–2.99
16	1	27.7	47.7	0.054	100	2.34	1.96–2.69
17	1	28.8	50.1	0.041	100	2.01	1.68–2.32
18	1	34.9	70.0	0.322	100	4.80	4.07–5.46
19	0.76	14.9	34.3	0.009	87	4.44	3.82–5.12
20	1	30.3	71.1	0.251	100	3.43	2.93–3.96
21	0.98	10.4	33.9	0.000	90	3.16	2.68–3.61
22	1	16.1	48.3	0.066	100	2.44	2.07–2.81
23	1	17.7	49.7	0.044	100	2.14	1.81–2.48
24	1	21.8	49.1	0.028	100	1.81	1.54–2.13
25	1	58.7	81.7	0.526	100	0.68	0.56–0.82
26	1	38.7	69.8	0.360	100	5.14	4.40–5.89
27	1	34.2	77.9	0.091	100	3.84	3.28–4.41
28	1	24.3	20.8	0.025	100	3.72	3.13–4.23
29	1	46.4	74.0	0.180	100	2.65	2.27–3.10
30	–	–	–	–	–	1.97	1.52–2.37
31	1	79.1	96.3	0.643	100	0.55	0.44–0.67
32	1	72.9	93.1	0.584	100	1.96	1.63–2.27
33	1	54.4	69.8	0.157	100	1.40	1.18–1.64

sister to all other *Chlorophonia* with reasonably high concordance factor support but low support from the IC index (gCF = 34.2, sCF = 77.9, IC = 0.091).

Three additional points in the mitogenome tree support relationships that were not found in any of the UCE-based phylogenies. First, *E. chrysopasta* was found to be sister to the set of 3 small *Euphonia* clades. This placement has only 74% bootstrap support in the mitochondrial phylogeny, but its placement in the 2 concatenated trees as the sister to (*minuta*, [*chalybea*, {*violacea*, (*hirundinacea*, *laniirostris*)}]) had 100% bootstrap support. Its placement in the ASTRAL species tree matched that of the 2 other UCE-based phylogenies, but had moderate to low concordance factor and IC support (gCF = 18.5, sCF = 47.7, IC = 0.093). We searched the individual gene tree topologies containing this relationship to find the frequency at which the UCE sequences supported this relationship and found that only 6.9% (107/1,558) of gene trees did. Second, *E. jamaica* and *saturata* are sister species in the mitochondrial tree with reasonably high bootstrap support (84%), whereas *jamaica* is sister to all other species in its lineage with high support in both the ASTRAL species tree (gCF = 34.9, sCF = 70.0, IC = 0.322) and the incomplete RAxML phylogeny (bootstrap = 100%), and *saturata* is sister to all other species within its clade in the complete, concatenated RAxML phylogeny with full bootstrap support. Only 18.1% (701/3,867) of individual UCE gene trees supported a sister relationship between the 2 species. Third, *E. chlorotica* diverges prior to *plumbea* within its respective clade, whereas the opposite is true in every other analysis of UCE loci. This arrangement received 100% bootstrap support, although the placement of *E. plumbea* received only 59% support, and the placement of *chlorotica* within this clade consistently received only moderate support in the concatenated (88 and 73%) and species tree (LPP = 0.98, gCF = 10.4, sCF = 33.9, IC = 0.000) analyses. Only 2.3% (61/2,597) of gene trees supported this arrangement. Overall, we found

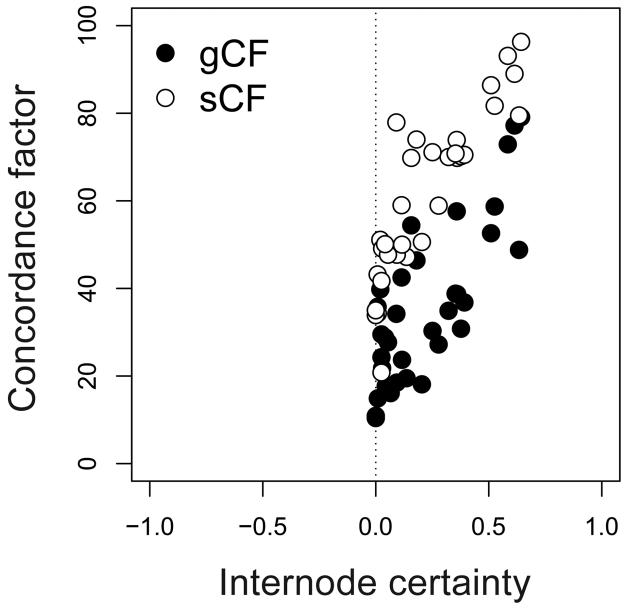

FIGURE 2. Internode certainty scores and concordance factors for the 4,944-locus ASTRAL species tree. Each point represents a node on the species tree, and the plot contains 2 full sets of points showing the gene and site concordance factors for each node in black and white, respectively. The dashed vertical line divides the plot in half: any points to the left of this line would indicate strong discordance of the gene trees and species tree for a particular node. While many points are on or directly adjacent to this line, no nodes in the species tree have negative internode certainties.

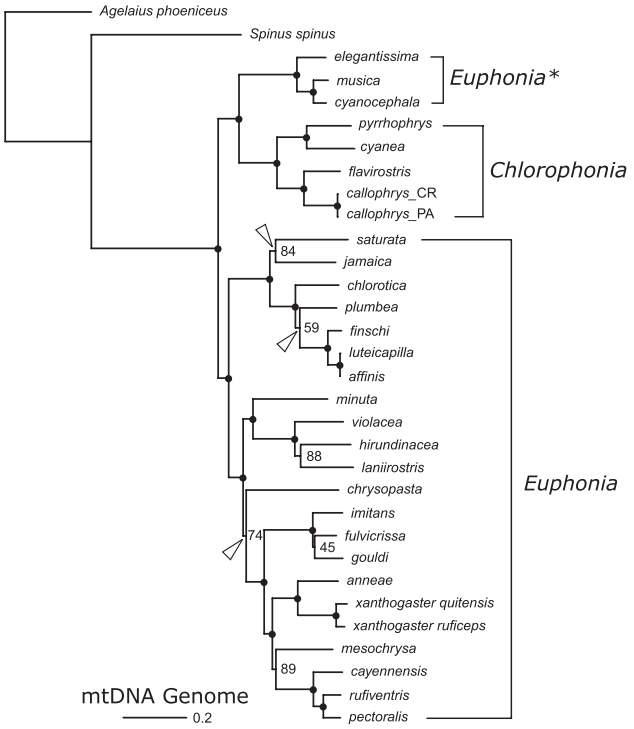

FIGURE 3. RAxML phylogeny inferred from partitioned mitochondrial genomes. Black circles indicate 100% bootstrap support for nodes along the tree, and only bootstrap supports <100% are shown adjacent to their respective nodes. White arrows point to 3 points on this phylogeny that differ from all of the UCE-based phylogenies: the sister relationship of *E. jamaica* and *saturata*, the placement of *E. chrysopasta*, and the placement of *E. chlorotica*. As in Figure 1, the blue-hooded *Euphonia* clade is marked with an asterisk.

evidence for only 3 instances of phylogenetic discordance between the mitochondrial and the nuclear UCE sequence data, with only moderate support.

Time-calibrated Bayesian Tree and Biogeographic Modeling

We extracted the full sequence of cytb from the mitochondrial genomes and used the sequence from *C. cyanea* to assemble the fragments of cytb that were sequenced from *C. occipitalis* into a single consensus sequence. The cytb alignment for this locus was 1,145 bp in length and was concatenated as the 120th partition in the sequence alignment for the BEAST2 analysis. After modifying the BEAST2 analysis, we drastically improved convergence on the prior and posteriors (ESS ≥ 3,000), so we generated our MCC tree from this posterior tree distribution to obtain the first species-level, time-calibrated phylogeny for this subfamily (Figure 4; see Appendix Figure 6 for the complete tree with outgroups). As expected given our prior, the stem node for the entire phylogeny representing the divergence of Emberizidae and Fringillidae was estimated to be 16.8 million years ago (mya) (95% HPD = 14.5–19.3 mya), congruent with the age estimate and HPD originally obtained from Oliveros et al. (2019). Above this node, we recover the split between Fringillinae and the rest of the fringillids ~14.6 mya (95% HPD = 12.4–16.5 mya), and the split between Euphoniinae and Carduelinae ~13.8 mya (95% HPD = 11.8–15.8 mya). A long branch spanning nearly 7 myr was recovered connecting the stem and crown nodes for Euphoniinae, with the crown age for this subfamily being much younger at only 7.1 mya (95% HPD = 6.0–8.0 mya). The crown node for the genus *Euphonia* (minus the blue-hooded species) occurs shortly after at 6.5 mya (95% HPD = 5.4–7.3 mya), and the crown nodes for *Chlorophonia* and the blue-hooded *Euphonia* are even younger at 3.8 mya (95% HPD = 3.3–4.4 mya) and 2.0 mya (95% HPD = 1.6–2.3 mya), respectively. Following these crown ages, speciation events appear quite evenly spaced through time, with the youngest speciation events occurring less than 1 mya, as in the case of *E. affinis* and *luteicapilla* (0.68 mya, 95% HPD = 0.56–0.82 mya).

Of the 3 biogeographic models fit to this tree, the DIVALIKE model was best-supported, although the DEC model fit these data comparably well (ΔAIC = 1.437). The actual biogeographic histories between these 2 models differed only marginally in that 3 nodes were reconstructed

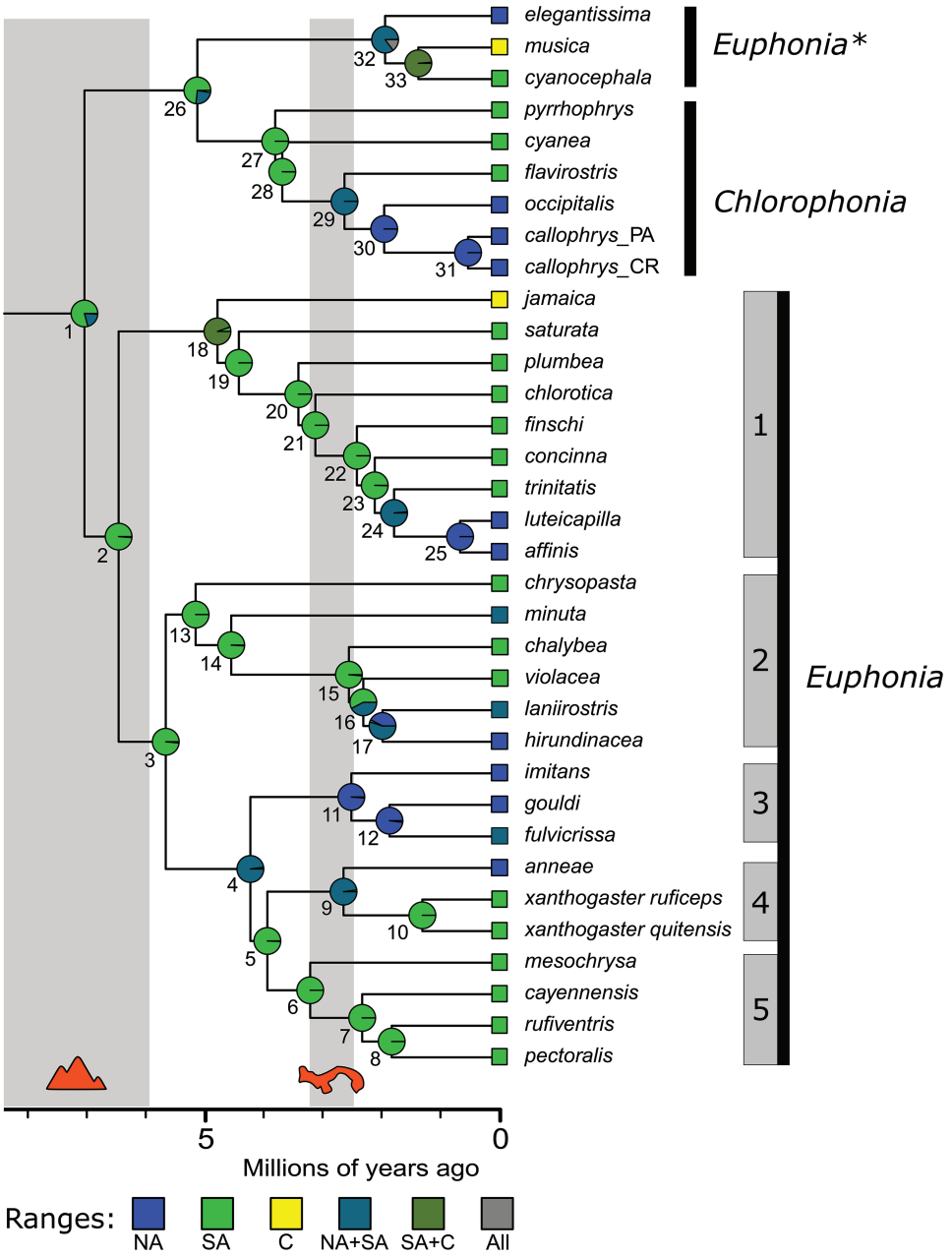

FIGURE 4. Biogeographic history and Bayesian time-scaled phylogeny of Euphoniinae. Node numbers correspond to the values of node support in Table 2, and the pie charts at each node show the proportional likelihood of possible ancestral ranges inferred by the DIVALIKE model. A legend describing these regions is given at the bottom with the following abbreviations: NA = North America, SA = South America, and C = Caribbean. Gray shaded regions along the phylogeny indicate 2 geologically significant time periods: the duration and end of Andean orogeny and the recently estimated age at which the Isthmus of Panama formed following O'Dea et al. (2016). Black lines delimit the euphoniine genera and gray bars adjacent to *Euphonia* delimit the clades that we describe in the Discussion. As previously, the blue-hooded euphonia clade is distinguished by the asterisk.

as being widespread North and South American in the DEC model and only South American in the DIVALIKE model, so here we focus on the DIVALIKE model results. In this model, the most likely ancestral range of crown Euphoniinae was South America, which was also the most likely ancestral range for the node uniting the blue-hooded euphonias and *Chlorophonia* and for the ancestral node of the remaining *Euphonia*. Beyond this initial period of diversification, all but 1 diversification event appeared to have occurred in South America until ~4 Ma, after which a number of nodes have inferred ranges occupying both North and South America. A total of 6 range expansion

events into North America from South America were inferred under this model: (1) the crown node of blue-hooded *Euphonia*; (2) the ancestor of *C. flavirostris, occipitalis*, and *callophrys*; (3) the ancestor of *E. trinitatis*, *luteicapilla*, and *affinis*; (4) the ancestor of *E. laniirostris* and *hirundinacea*; (5) the ancestral node for the 3 small *Euphonia* clades; and (6) within the small *Euphonia* clades, the ancestor of *E. anneae* and *xanthogaster*. Additionally, 2 nodes were inferred to have ranges occupying both South America and some region of the Caribbean, and both of these nodes give rise to a single species currently found in the Caribbean on 1 side of the split and at least 1 South American species or node on the other side. However, these nodes leading to species occurring in the Caribbean were not temporally clustered like the South to North America range shifts and occur at 4.8 and 1.4 mya for *E. jamaica* and *E. musica*, respectively. Taken together, the DIVALIKE model of biogeographic range evolution showed a consistent South American origin for the euphoniine lineage that repeatedly expanded northward and dispersed twice to islands of the Caribbean.

The results of the lesser supported DEC model suggest that 3 ancestors: (1) the ancestral node for Euphoniinae; (2) the node uniting *Chlorophonia* and blue-hooded euphonias; and (3) the node uniting *Euphonia anneae* + *xanthogaster* with *E. mesochrysa*, *cayennensis*, *rufiventris*, and *pectoralis*, occupied both North and South America, instead of only South America as in the DIVALIKE model. This biogeographic scenario implies only 4 range expansions from South America into North America instead of 6, but the same South America to Caribbean range expansions were inferred and the remainder of the biogeographic history inferred from this model is nearly identical to that of the DIVALIKE model.

DISCUSSION

Congruence of Phylogenomic Analyses and Previous Classifications

In this study, we applied molecular systematic methods to resolve the taxonomic relationships among the genera and species in the passerine subfamily Euphoniinae and used this phylogenetic framework to model the biogeographic history and timing of diversification within this unusual group of birds. Combining a well-developed target enrichment and sequencing pipeline with species-level sampling allowed us to infer the first species-level phylogeny for this subfamily with orders of magnitude more sequence data than previous studies. The phylogenetic hypotheses inferred from nearly 5,000 nuclear UCE loci and complete mitochondrial genomes using both concatenated and coalescent-based methods are largely congruent and effectively resolve the genus- and species-level relationships of *Euphonia* and *Chlorophonia*.

We found that all recognized species in the subfamily form a young, monophyletic lineage sister to outgroup representatives (*Spinus* and *Coccothraustes*) from the sister subfamily Carduelinae, confirming that Euphoniinae is a sound taxon. Immediately after the basal divergence of this lineage, we recover a divergence event that separates blue-hooded *Euphonia* species and *Chlorophonia* from the remaining *Euphonia* species, a relationship originally suggested by Zuccon et al. (2012) with a smaller sample of taxa. By including all species in this phylogeny, we confirmed that all 3 blue-hooded *Euphonia* species form a monophyletic lineage that is sister to the 5 *Chlorophonia* species with uniformly high support in every phylogenetic analysis, demonstrating that the genus *Euphonia*, as currently delimited, is paraphyletic with regard to *Chlorophonia*. We address the need for revising taxonomic limits of these genera and offer a resolution to this issue below. Within the blue-hooded *Euphonia* clade, every analysis recovered *E. elegantissima* as sister to *musica* and *cyanocephala*, and relationships within *Chlorophonia* varied only in the placement of *pyrrhophrys*. Every concatenation-based analysis of both the UCE and mitochondrial sequences infer a sister relationship between *C. pyrrhophrys* and *cyanea* to the exclusion of the other 3 species with high bootstrapping support, whereas the species tree analysis places *C. pyrrhophrys* as the sister to all other species within the genus, albeit with a short branch and with moderate to low IC support (0.091). These results suggest that the early diversification events within this genus may have happened rapidly.

Similar to Isler and Isler's (1999) treatment of *Euphonia*, our results support 5 clades within the genus that, with the exception of 1 species in the mitochondrial tree (*E. chrysopasta*), are found and well-supported in each phylogeny we inferred in this study. The first and largest clade we describe here contains the species *E. jamaica*, *saturata*, *plumbea*, *chlorotica*, *finschi*, *concinna*, *trinitatis*, *luteicapilla*, and *affinis*, and is an amalgamation of groups 1 and 2 sensu Isler and Isler. The only variable placements of any species in this clade are the oldest divergences defining the placement of *E. jamaica, saturata,* and *chlorotica*. The second clade we define includes the species *E. chrysopasta*, *minuta*, *chalybea*, *violacea*, *laniirostris*, and *hirundinacea*, and includes species from Isler and Isler's species groups 3, 5, and 6. Relationships within this clade were uniformly resolved across analyses with the exception of *E. chrysopasta*'s placement in the mitochondrial genome tree as the sister taxon to the next 3 *Euphonia* clades. But the placement of this taxon at this point or within our second clade never received maximum support values in any phylogenetic analysis.

The last 3 clades we identified across our phylogenies form a monophyletic group in each tree, although the relationships between these 3 clades are some of the

most variable points in the phylogeny of the entire subfamily. The concatenated phylogenies inferred from the 4,956 concatenated UCE loci and from the mitochondrial genomes plus the species tree inferred from the incomplete UCE matrix placed our third clade, containing the species *E. imitans*, *gouldi*, and *fulvicrissa*, as sister to the remaining 2 clades at this point in the tree. Excepting the exclusion of *E. chrysopasta* and *mesochrysa*, this clade is identical to Isler and Isler's group 5. Only the RAxML phylogeny inferred from the 150 concatenated and partitioned UCE loci proposed a different relationship among these 3 small clades in which our fourth clade, which is identical to Isler and Isler's group 7 and contains only *E. anneae* and *xanthogaster*, was sister to the other 2. Within this clade, we found surprisingly deep divergences between the 2 subspecies of *E. xanthogaster* in this study, and the significance of this result, along with its implications of potentially undescribed species-level diversity, are discussed below. Lastly, our fifth clade, which includes 4 species, *E. mesochrysa*, *cayennensis*, *rufiventris*, and *pectoralis*, has uniformly resolved relationships in every phylogeny, and is congruent with Isler and Isler's species group 8 except with the addition of *mesochrysa*.

Altogether, our phylogenetic hypotheses inferring the relationships within the subfamily Euphoniinae are largely concordant with one another and with previous taxonomic treatments of this group. With few exceptions, we recover the species groups defined by Isler and Isler in their classification of the genera with the only differing relationships inferred in our study involving species that were not concretely placed in their classification. At a higher level, the obvious exception to this concordance is Isler and Isler's species group 4, containing the blue-hooded euphonias, which we recover as sister to *Chlorophonia* and outside of *Euphonia*. With complete sampling and the analytical power afforded by our data, it is now possible and necessary to revise the generic taxonomy of these birds with 3 plausible alternative solutions outlined below.

Paraphyly of *Euphonia* and Historical Precedent for Three Genera of Euphoniine Finches

Here we present 3 potential taxonomic revisions that would resolve the paraphyly of *Euphonia*: (1) lump all species in the subfamily Euphoniinae into *Euphonia*, (2) add the blue-hooded euphonias to *Chlorophonia*, or (3) resurrect the previously described genus *Cyanophonia* for the blue-hooded euphonias. The genus *Euphonia* was established by Anselme-Gaëton Desmarest in 1806 in his *Histoire naturelle des Tangaras, des Manakins et des Todiers* and, thus, has priority over the genus *Chlorophonia*, which was described by Charles Lucien Bonaparte in 1851 in the second series and third volume of the *Revue et Magasin de Zoologie Pure et Appliquée*. While this priority lends support to the first proposed solution, the dissolution of *Chlorophonia* and lumping all species under *Euphonia* would remove a comparably long-standing genus and overturn 168 yr of recognition of the former genus. The second proposed solution would require the revision of 3 species binomials, rather than 5 in the first solution, but given that only females of the blue-hooded euphonia species and males in some populations of *E. musica* in the Lesser Antilles possess any green plumage as adults, the name *Chlorophonia* does not describe the phenotypes of these species particularly well. The third proposal stems from the fact that, in the same work in which he created the name *Chlorophonia*, Bonaparte also designated a separate genus for *E. musica* and *cyanocephala* (then described as *aureata*): "*Nous donnons plus particulièrement le nom de CYANOPHONIA aux Euphones à tête bleue* [More specifically we give the name CYANOPHONIA to the blue-headed Euphonias]" (Bonaparte, 1851). Because the name *Cyanophonia* has equal priority to *Chlorophonia* and was specifically given to describe the blue-hooded species as distinct from other euphonias and the chlorophonias, we recommend resurrecting this genus and assigning the blue-hooded euphonias to this genus. Additionally, this solution requires revising only 3 taxon names and will result in a descriptive generic name for them. Despite the description of this genus in 1851, to our knowledge, a type species has never been formally designated for the genus *Cyanophonia*. Of the 3 recognized species in this genus, *musica* was described by Johann Friedrich Gmelin in part 2 of the 13th edition of *Systema Naturae* (1789) and is older than both *cyanocephala* (1819) and *elegantissima* (1838). Therefore, we designate the Antillean Euphonia, *Cyanophonia musica* (Linnaeus and Gmelin 1789), as the type species for the genus.

Biogeographic History of Euphoniinae

Given the present-day distribution of the family Fringillidae and closely related passerine families, in addition to the biogeographic analyses performed in this study, we conclude that the euphoniine lineage dispersed to the Western Hemisphere from Eurasia during the mid- to late-Miocene between 13.8–7.1 mya. As described above, modern members of this lineage are distinct ecologically when compared with most other finches, so it is likely that this lineage dispersed from the Eastern Hemisphere and evolved these unique adaptations from an ancestral nomadic, granivorous phenotype during this 7 myr time frame. But by what route did this ancestral population arrive in the Americas? The vast majority of passerine dispersal events from the Eastern into the Western Hemisphere appear to have taken place through Beringia (Cracraft 1973, Barker et al. 2004), which facilitated overland dispersal into North America throughout most of the Cenozoic until the latest Miocene and Pliocene between 7.4 and 4.8 mya and then sporadically throughout the Pleistocene (Hopkins 1967, Marincovich and Gladenkov 1999). Although

rarer, transoceanic dispersal events from Eurasia or Africa into the Americas, especially South America, have repeatedly occurred in a number of passerine lineages (*Anthus*, Voelker 1999; *Turdus*, Voelker et al. 2009; *Donacobius,* Fregin et al. 2012), in pelecaniform birds (*Bubulcus ibis,* Crosby 1972; *Plegadis falcinellus,* Oswald et al. 2019), and even in 2 orders of mammals (Primates and Rodentia, Simpson 1980). Many extant finch species are long-distance migrants and many others (euphonias included) are nomadic throughout their annual cycles, which has led to their colonization of isolated oceanic islands like the Azores, Canaries, and Madeira by *Fringilla* (Marshall and Baker 1999), and the Hawaiian archipelago by the ancestor of the honeycreepers (Lerner et al. 2011). Considering these confamilial examples of long-distance oceanic dispersal with the *BioGeoBEARS* results from this study, transoceanic dispersal from the Eastern Hemisphere to South America is indeed a possible, and perhaps even likely, means of arrival for Euphoniinae into the Americas. An alternative scenario, supported by the DEC model inferred from these data, proposes that the ancestral population giving rise to Euphoniinae was widespread in both North and South America. It is possible that the ancestral population could have dispersed to either North or South America over water or over land, expanded its range to occupy both continents, and underwent range contractions or extinctions within both *Euphonia* and *Chlorophonia*, only leaving descendants in South America. Given the variability in age estimates at which North and South America became one contiguous landmass (discussed below), we cannot rule out this scenario despite it not being selected as the one best-fitting the phylogeny and contemporary range data.

Following dispersal into the Western Hemisphere, both *Euphonia* and *Chlorophonia* apparently diversified in South America, while we infer that *Cyanophonia* remained widespread throughout North and South America until 1.8 mya, around which time it diversified. Species in this genus typically inhabit forests and other habitats where mistletoes (Santalales) are common, and their speciation during the Pleistocene may have been vicariant—driven by climate cycles that repeatedly shifted and isolated patches of such forests—with *elegantissima* diverging first in North America, followed by *musica* and *cyanocephala* in the Caribbean and South America, respectively. Interestingly, within *Euphonia* and in *Chlorophonia*, we found that all lineages presently occurring in North America evolved from South American ancestors. Assuming these lineages had evolved the strongly frugivorous and nonmigratory habits of modern species by their crown age, all these dispersal events likely required continuous expanses of tropical forest connecting both continents in order to take place. Such expanses of continuous habitat could only exist on a completely formed Isthmus of Panama. A substantial research effort spanning the fields of geology, paleobiology, and phylogenetics has focused on resolving the time frame over which the Central American Seaway closed and the Isthmus of Panama fully formed, with estimates ranging from older than 20 mya (Bacon et al. 2015), to the mid-Miocene around 13–10 mya (Montes et al. 2015), and as young as 2.8 mya (Coates and Obando 1996, O'Dea et al. 2016). The divergence times for each of the species and clades found in North America ranges from 4.3 to 1.8 mya, with the upper bound of the 95% HPD for any of these nodes extending to 4.9 mya. Assuming that these lineages dispersed northward as soon as adequate habitat was available and the route was traversable, which was likely the case in both North and South America by this time frame (Graham 1987a,b, Behrensmeyer et al. 1992, Jaramillo et al. 2014), our data support a younger age for the formation of the isthmus and corroborate previous findings that avian dispersal between North and South America reached its maximum frequency during the Pliocene (Bacon et al. 2015, Barker et al. 2015).

Additionally, our biogeographic modeling results clearly show 2 spatially and temporally independent dispersal events of a single species into the Caribbean from a South American ancestor, *Cyanophonia musica* and *Euphonia jamaica.* A large body of literature has investigated the biogeographic history of the Caribbean and the avenues by which this region has accumulated its biodiversity. Recent work describing the historical biogeography of both terrestrial mammals and birds has shown that dispersal to the islands of the Caribbean from South America is a prevalent and likely scenario for these broad taxonomic groups (Dávalos 2004, Ricklefs and Bermingham 2008). The geographic landscape of the Caribbean strongly resembled its modern state by ~5 mya, at which time substantial tectonic uplift had led to the emergence of the majority of islands and, thus, could facilitate shorter distance dispersal events in a stepping-stone manner between landmasses (Perfit and Williams 1989). Given the absence of land bridges connecting South America to any of the Caribbean islands since the late Oligocene (Iturralde-Vinent and MacPhee 1999) and that both diversification events producing these species occurred after 5 mya, island-hopping and over-water dispersal appear to be the only possible route by which these 2 species could have come to occupy their current ranges. This explanation is especially convincing for *Cyanophonia musica*, which is found on most of the Lesser Antilles, Puerto Rico, and Hispaniola, and whose sister species is the widespread South American species *C. cyanocephala*, implying that this species may have expanded northward via successive northward colonization of islands from the mainland.

Potentially Unrecognized Species-level Diversity

Another notable outcome of this study was the finding that the magnitude of sequence and time divergence between the 2 subspecies of *E. xanthogaster* examined here is as great as, or even greater than, that observed between some other

sister species in the tree. *E. xanthogaster* exhibits striking phenotypic variation throughout its extensive range in South America (Olson 1981), where populations in the northern Maritime Andes (subspecies *exsul* and *badissima*) and in La Paz and Cochabamba Bolivia (subspecies *ruficeps*) have rufous crowns and orange ventral plumage, and, throughout the remainder of this species' range, the crown and ventral plumage is yellow (including subspecies *quitensis* and the allopatric subspecies *xanthogaster* in the Atlantic Forest; Isler and Isler 1999). Although this species is sexually dimorphic, these phenotypic differences in crown and ventral plumage are found to some extent in both males and females. Considering the genetic and phenotypic distinctiveness of the subspecies included in this study, this suggests that a thorough population-level study of genetic and phenotypic divergence of this species may reveal undescribed species-level diversity in *E. xanthogaster* across the continent of South America.

Similar circumstances of allopatric and phenotypically distinctive subspecies are documented in several other species, including *C. cyanea*, *E. affinis* (Dickerman 1981), *E. cyanocephala*, *E. laniirostris*, and *E. musica* (Isler and Isler 1999, del Hoyo et al. 2019). A lineages-through-time plot generated from our ultrametric MCC tree shows a plateauing of species diversification toward the present and a significant, negative γ value (–3.758, $P < 0.001$) that can be interpreted in 2 ways (Appendix Figure 7). First, it is possible that Euphoniinae underwent rapid, early diversification that has slowed down toward the present in a density-dependent manner (Pybus and Harvey 2000, Rabosky 2009). Or second, and perhaps more likely given our findings with *E. xanthogaster* and our observations of other wide-ranging phenotypically disparate taxa, this plateauing of species diversification toward the present is an artifact of failing to account for undescribed species-level diversity within this lineage. Investigating potentially undescribed species-level diversity within this lineage and testing which scenario best explains the accumulation of lineages through time for this group will require much denser sampling and is beyond the scope of the present study.

CONCLUSIONS

The taxonomic placement and relationships within the subfamily Euphoniinae (Passeriformes: Fringillidae) have changed substantially in the last 20 yr as the use of molecular systematics has become more widespread. Previously placed in the family Thraupidae because of their superficial similarity, subsequent systematic work showed that the 2 genera, *Euphonia* and *Chlorophonia*, are nested within the true finch family Fringillidae and that the genus *Euphonia* is paraphyletic. Using next-generation target capture and sequencing of thousands of UCE loci and complete mitochondrial genomes, we have inferred the first species-level phylogeny for the subfamily with concatenated and coalescent-based methods using ML and Bayesian approaches. We definitively show that *Euphonia* is paraphyletic with regard to *Chlorophonia* and recommend that the 3 blue-hooded euphonias be reassigned to a previously described genus, *Cyanophonia*, with *Cyanophonia musica* representing the type species of the genus. Within the genera, species-level relationships were largely resolved with few exceptions, and we define 5 clades within the genus *Euphonia* that are largely concordant with previous groupings according to phenotypic and behavioral similarity. By comparing ML models of biogeographic range evolution on an ultrametric time-calibrated species tree, we resolved the biogeographic history of the subfamily Euphoniinae. Specifically, we found that this lineage is relatively quite young and likely underwent a transoceanic dispersal event from the Eastern Hemisphere into South America in a 7 myr window between 13.8 and 7.1 mya, followed by 2 independent overwater dispersal events from South America to islands in the Caribbean and 6 dispersal events from South America into North America that correspond to the estimated timing at which the Isthmus of Panama had completely formed and permitted overland dispersal. Lastly, we found that 2 phenotypically disparate and allopatric subspecies of *E. xanthogaster* are more genetically divergent than other recognized sister species and likely represent one of several instances within the subfamily in which there is undescribed species-level diversity. We encourage subsequent studies to increase sampling efforts at subspecific and population levels to thoroughly investigate this possibility and to more concretely resolve the taxonomy and biogeographic history of this unique and fascinating group of Neotropical birds.

ACKNOWLEDGMENTS

This study would not have been possible without natural history collections and the people who make these resources available for research. We especially thank the curators and collection managers of the Louisiana State University Museum of Natural Science (LSUMZ), Field Museum of Natural History (FMNH), Yale Peabody Museum (YPM), Museum of Vertebrate Zoology at University of California, Berkeley (MVZ), United States National Museum of Natural History (USNM), and Bell Museum at the University of Minnesota (MMNH) for loaning us the specimens used in this study.

Funding statement: This research was funded by a Frank Chapman Memorial Grant from the American Museum of Natural History (AMNH), a Richard & Judie Huempfner Avian Research Grant from the Bell Museum, and a grant from the National Science Foundation (DEB-1541312).

Ethics statement: All specimens were collected under permits to corresponding institutions.

Author contributions: T.S.I. conceived of the research, conducted all lab work, performed the bioinformatic and phylogenomic analyses, and wrote the paper. F.K.B. contributed substantially to the analyses and to writing the paper. R.T.B. also contributed to writing the paper.

Data availability: The mitogenome sequences from this project have been deposited in GenBank's nucleotide archive (accession IDs: MT063155–MT063184) and the raw Illumina read data have been deposited in the NCBI Short Read Archives (BioProject ID: PRJNA604822). Alignments, tree files, and metadata are deposited in the Dryad Digital Repository (Imfeld et al. 2020).

LITERATURE CITED

Andersen, M. J., J. M. McCullough, N. R. Friedman, A. T. Peterson, R. G. Moyle, L. Joseph, and Á. S. Nyári (2019). Ultraconserved elements resolve genus-level relationships in a major Australasian bird radiation (Aves: Meliphagidae). Emu 119:218–232.

Bacon, C. D., D. Silvestro, C. Jaramillo, B. T. Smith, P. Chakrabarty, and A. Antonelli (2015). Biological evidence supports an early and complex emergence of the Isthmus of Panama. Proceedings of the National Academy of Sciences of the United States of America 112:6110–6115.

Barker, F. K., A. J. Vandergon, and S. M. Lanyon (2008). Assessment of species limits among Yellow-breasted Meadowlarks (*Sturnella* spp.) using mitochondrial and sex-linked markers. The Auk 125:869–879.

Barker, F. K., K. J. Burns, J. Klicka, S. M. Lanyon, and I. J. Lovette (2013). Going to extremes: Contrasting rates of diversification in a recent radiation of New World passerine birds. Systematic Biology 62:298–320.

Barker, F. K., K. J. Burns, J. Klicka, S. M. Lanyon, and I. J. Lovette (2015). New insights into New World biogeography: An integrated view from the phylogeny of blackbirds, cardinals, sparrows, tanagers, warblers, and allies. The Auk: Ornithological Advances 132:333–348.

Barker, F. K., A. Cibois, P. Schikler, J. Feinstein, and J. Cracraft (2004). Phylogeny and diversification of the largest avian radiation. Proceedings of the National Academy of Sciences of the United States of America 101:11040–11045.

Behrensmeyer, A. K., J. D. Damuth, W. A. DiMichele, R. Potts, H.-D. Sues, and S. L. Wing (1992). Terrestrial Ecosystems Through Time: Evolutionary Paleoecology of Terrestrial Plants and Animals. 2nd edition. University of Chicago Press, Chicago, IL, USA.

Bonaparte, C. L. (1851). Note sur les Tangaras, leurs affinités, et descriptions d'espèces nouvelles. Revue et Magasin de Zoologie Pure et Appliquée 2:129–138.

Bouckaert, R., J. Heled, D. Kühnert, T. Vaughan, C. H. Wu, D. Xie, M. A. Suchard, A. Rambaut, and A. J. Drummond (2014). BEAST 2: A software platform for Bayesian evolutionary analysis. Plos Computational Biology 10:e1003537.

Bryson, R. W., B. C. Faircloth, W. L. E. Tsai, J. E. McCormack, and J. Klicka (2016). Target enrichment of thousands of ultraconserved elements sheds new light on early relationships within New World sparrows (Aves: Passerellidae). The Auk: Ornithological Advances 133:451–458.

Burns, K. J. (1997). Molecular systematics of tanagers (Thraupinae): Evolution and biogeography of a diverse radiation of neotropical birds. Molecular Phylogenetics and Evolution 8:334–348.

Burns, K. J., S. J. Hackett, and N. K. Klein (2003). Phylogenetic relationships of Neotropical honeycreepers and the evolution of feeding morphology. Journal of Avian Biology 34:360–370.

Burns, K. J., A. J. Shultz, P. O. Title, N. A. Mason, F. K. Barker, J. Klicka, S. M. Lanyon, and I. J. Lovette (2014). Phylogenetics and diversification of tanagers (Passeriformes: Thraupidae), the largest radiation of Neotropical songbirds. Molecular Phylogenetics and Evolution 75:41–77.

Cibois, A. (2003). Mitochondrial DNA phylogeny of babblers (Timaliidae). The Auk 120:35–54.

Cibois, A., and J. Cracraft (2004). Assessing the passerine "Tapestry": Phylogenetic relationships of the Muscicapoidea inferred from nuclear DNA sequences. Molecular Phylogenetics and Evolution 32:264–273.

Chesser, R. T., K. J. Burns, C. Cicero, J. L. Dunn, A. W. Kratter, I. J. Lovette, R. C. Rasmussen, J. V. Remsen, D. F. Jr. Stotz, B. M. Winger, and K. Winker (2018). Check-list of North American Birds (online). American Ornithological Society https://checklist.aou.org/taxa

Coates, A. G., and J. A. Obando (1996). The Geologic Evolution of the Central American Isthmus. In Evolution and Environment in Tropical America (J. B. C. Jackson, A. F. Budd, and A. G. Coates, Editors). University of Chicago Press, Chicago, IL, USA. pp. 21–56.

Cracraft, J. (1973). Continental drift, paleoclimatology, and the evolution and biogeography of birds. Journal of Zoology 169:455–545.

Dávalos, L. M. (2004). Phylogeny and biogeography of Caribbean mammals. Biological Journal of the Linnean Society 81:373–394.

Desmarest, A. G. (1806). Histoire naturelle des Tangaras, des Manakins et des Todiers. folio Paris.

Desselberger, H. (1931). Der Verdauungskanal der Dicaeiden nach Gestalt und Funktion. Journal of Ornithology 79:353–370.

del Hoyo, J., A. Elliot, J. Sargatal, D. A. Christie, and G. Kirwan (Editors) (2019). Handbook of the Birds of the World Alive. Lynx Edicions, Barcelona, Spain. https://www.hbw.com/.

Dickerman, R. W. (1981). Geographic Variation in the Scrub Euphonia. Occasional Papers of the Museum of Zoology 59:1–6.

Faircloth, B. C. (2013). Illumiprocessor: A Trimmomatic wrapper for parallel adapter and quality trimming. http://illumiprocessor.readthedocs.io/en/latest/index.html.

Faircloth, B. C. (2016). PHYLUCE is a software package for the analysis of conserved genomic loci. Bioinformatics 32:786–788.

Faircloth, B. C., J. E. McCormack, N. G. Crawford, M. G. Harvey, R. T. Brumfield, and T. C. Glenn (2012). Ultraconserved elements anchor thousands of genetic markers spanning multiple evolutionary timescales. Systematic Biology 61:717–726.

Forbes, W. A. (1880). Contributions to the anatomy of passerine birds–Part I. On the structure of the stomach in certain genera

of tanagers. Proceedings of the Zoological Society of London 143–147.
Fregin, S., M. Haase, U. Olsson, and P. Alström (2012). New insights into family relationships within the avian superfamily Sylvioidea (Passeriformes) based on seven molecular markers. BMC Evolutionary Biology 12:157.
Gelang, M., A. Cibois, E. Pasquet, U. Olsson, P. Alström, and P. G. P. Ericson (2009). Phylogeny of babblers (Aves, Passeriformes): Major lineages, family limits and classification. Zoologica Scripta 38:225–236.
Gill, F., and D. Donsker (Editors) (2019). IOC World Bird List (v9.2). doi:10.14344/IOC.ML.9.2.
Graham, A. (1987a). Miocene communities and paleoenvironments of southern Costa Rica. American Journal of Botany 74:1501–1518.
Graham, A. (1987b). Tropical American tertiary floras and paleoenvironments: Mexico, Costa Rica, and Panama. American Journal of Botany 74:1519–1531.
Hartert, E. (1910). Die Vögel der paläarktischen Fauna systematische Übersicht der in Europa, Nord-Asien under der Mittelmeerregion vorkommenden Vögel. 1st edition. R Friedländer und Sohn, Berlin, Germany.
Hasegawa, M., H. Kishino, and T. Yano (1985). Dating of the human-ape splitting by a molecular clock of mitochondrial DNA. Journal of Molecular Evolution 22:160–174.
Hellmayr, C. E. (1936). Catalogue of birds of the Americas and the adjacent Islands. Tersinidae-Thraupidae. Field Museum of Natural History Publication Zoological Series 13:1–458.
Hopkins, D. M. (1967). The Bering Land Bridge. Stanford University Press, Stanford, CA, USA.
Imfeld, T. S., F. K. Barker, and R. T. Brumfield (2020). Data from: Mitochondrial genomes and thousands of ultraconserved elements resolve the taxonomy and historical biogeography of the *Euphonia* and *Chlorophonia* finches (Passeriformes: Fringillidae). The Auk: Ornithological Advances 137:1–25. doi:10.5061/dryad.6t1g1jwvv.
Isler, M. L., and P. R. Isler (1999). The Tanagers: Natural History, Distribution, and Identification. 2nd edition. Smithsonian Institution Press, Washington, DC, USA.
Iturralde-Vinent, M. A., and R. MacPhee (1999). Paleogeography of the Caribbean region: Implications for cenozoic biogeography bulletin of the American Museum of Natural History. Bulletin of the American Museum of Natural History 238:1–95.
Jaramillo, C., E. Moreno, V. Ramírez, S. da Silva, A. de la Barrera, A. de la Barrera, C. Sánchez, S. Morón, F. Herrera, J. Escobar, et al. (2014). Palynological record of the last 20 million years in Panama. In Paleobotany and Biogeography: A Festschrift for Alan Graham in his 80th Year (W. D. Stevens, P. H. Raven, and O. M. Montiel, Editors). Missouri Botanical Garden, MO, USA. pp. 134–251.
Jønsson, K. A., M. P. K. Blom, P. Z. Marki, L. Joseph, G. Sangster, P. G. P. Ericson, and M. Irestedt (2019). Complete subspecies-level phylogeny of the Oriolidae (Aves: Passeriformes): Out of Australasia and return. Molecular Phylogenetics and Evolution 137:200–209.
Klicka, J., K. P. Johnson, and S. M. Lanyon (2000). New World nine-primaried oscine relationships: Constructing a mitochondrial DNA framework. The Auk 117:321–336.
Lanfear, R., P. B. Frandsen, A. M. Wright, T. Senfeld, and B. Calcott (2017). PartitionFinder 2: New methods for selecting partitioned models of evolution for molecular and morphological phylogenetic analyses. Molecular Biology and Evolution 34:772–773.
Lerner, H. R., M. Meyer, H. F. James, M. Hofreiter, and R. C. Fleischer (2011). Multilocus resolution of phylogeny and timescale in the extant adaptive radiation of Hawaiian Honeycreepers. Current Biology 21:1838–1844.
Linnaeus, C., and J. F. Gmelin (1789). Systema naturae per regna tria naturae. Impensis Georg Emmanuel Beer, Leipzig, Germany.
Marincovich, L., and A. Y. Gladenkov (1999). Evidence for an early opening of the Bering Strait. Nature 397:149–151.
Marshall, H. D., and A. J. Baker (1999). Colonization history of Atlantic Island Common Chaffinches (*Fringilla coelebs*) revealed by mitochondrial DNA. Molecular Phylogenetics and Evolution 11:201–212.
Matzke, N. J. (2013a). Probabilistic historical biogeography: New models for founder-event speciation, imperfect detection, and fossils allow improved accuracy and model-testing. Frontiers of Biogeography 5. http://escholarship.org/uc/item/44j7n141.
Matzke, N. J. (2013b). BioGeoBEARS: Biogeography with Bayesian (and likelihood) evolutionary analysis in R scripts. CRAN: The Comprehensive R Archive Network, Berkeley, CA, USA. https://CRAN.R-project.org/package=BioGeoBEARS.
Mayr, E., and D. Amadon (1951). A classification of recent birds. American Museum Novitates 1946:1–42.
McCormack, J. E., M. G. Harvey, B. C. Faircloth, N. G. Crawford, T. C. Glenn, and R. T. Brumfield (2013). A phylogeny of birds based on over 1,500 loci collected by target enrichment and high-throughput sequencing. Plos One 8:e54848.
Miller, M. A., W. Pfeiffer, and T. Schwartz (2010). Creating the CIPRES Science Gateway for inference of large phylogenetic trees. Proceedings of the Gateway Computing Environments Workshop (GCE), November 14, 2010, New Orleans, LA, USA. pp. 1–8.
Minh, B. Q., M. W. Hahn, and R. Lanfear (2018). New methods to calculate concordance factors for phylogenomic datasets. bioRxiv doi: 10.1101/487801.
Montes, C., A. Cardona, C. Jaramillo, A. Pardo, J. C. Silva, V. Valencia, C. Ayala, L. C. Pérez-Angel, L. A. Rodriguez-Parra, V. Ramirez, and H. Niño (2015). Middle Miocene closure of the Central American Seaway. Science 348:226–229.
Moyle, R. G., C. H. Oliveros, M. J. Andersen, P. A. Hosner, B. W. Benz, J. D. Manthey, S. L. Travers, R. M. Brown, and B. C. Faircloth (2016). Tectonic collision and uplift of Wallacea triggered the global songbird radiation. Nature Communications 7:12709.
Musher, L. J., and J. Cracraft (2018). Phylogenomics and species delimitation of a complex radiation of Neotropical suboscine birds (*Pachyramphus*). Molecular Phylogenetics and Evolution 118:204–221.
Nguyen, L. T., H. A. Schmidt, A. von Haeseler, and B. Q. Minh (2015). IQ-TREE: A fast and effective stochastic algorithm for estimating maximum-likelihood phylogenies. Molecular Biology and Evolution 32:268–274.
O'Dea, A., H. A. Lessios, A. G. Coates, R. I. Eytan, S. A. Restrepo-Moreno, A. L. Cione, L. S. Collins, A. de Queiroz, D. W. Farris, R. D. Norris, et al. (2016). Formation of the Isthmus of Panama. Science Advances 2:e1600883.
Oliveros, C. H., D. J. Field, D. T. Ksepka, F. K. Barker, A. Aleixo, M. J. Andersen, P. Alström, B. W. Benz, E. L. Braun, M. J. Braun,

et al. (2019). Earth history and the passerine superradiation. Proceedings of the National Academy of Sciences of the United States of America 116:7916–7925.

Olson, S. (1981). A revision of the northern forms of *Euphonia xanthogaster* (Aves: Thraupidae). Proceedings of the Biological Society of Washington 94:101–106.

Oswald, J. A., M. G. Harvey, R. C. Remsen, D. U. Foxworth, D. L. Dittmann, S. W. Cardiff, and R. T. Brumfield (2019). Evolutionary dynamics of hybridization and introgression following the recent colonization of Glossy Ibis (Aves: *Plegadis falcinellus*) into the New World. Molecular Ecology 28:1675–1691.

Paradis, E., J. Claude, and K. Strimmer (2004). APE: Analyses of Phylogenetics and Evolution in R language. Bioinformatics 20:289–290.

Pérez-Rivera, R. (1991). Change in diet and foraging behavior of the Antillean Euphonia in Puerto Rico after Hurricane Hugo. Journal of Field Ornithology 62:474–478.

Perfit, M., and E. E. Williams (1989). Geological constraints and biological retrodictions in the evolution of the Caribbean sea and its islands. In Biogeography of the West Indies: Past, Present, and Future (C. A. Woods, Editor). Sandhill Crane Press, Gainesville, FL, USA. pp. 47–102.

Powell, A. F. L. A., F. K. Barker, and S. M. Lanyon (2013). Empirical evaluation of partitioning schemes for phylogenetic analyses of mitogenomic data: An avian case study. Molecular Phylogenetics and Evolution 66:69–79.

Pybus, O. G., and P. H. Harvey (2000). Testing macro-evolutionary models using incomplete molecular phylogenies. Proceedings. Biological Sciences 267:2267–2272.

R Core Team. (2013). R: A Language and Environment for Statistical Computing. R Foundation for Statistical Computing, Vienna, Austria. http://www.R-project.org/

Rabosky, D. L. (2009). Ecological limits and diversification rate: Alternative paradigms to explain the variation in species richness among clades and regions. Ecology Letters 12:735–743.

Rambaut, A., A. J. Drummond, D. Xie, G. Baele, and M. A. Suchard (2018). Posterior summarization in Bayesian phylogenetics using tracer 1.7. Systematic Biology 67:901–904.

Reddy, S., and J. Cracraft (2007). Old World Shrike-babblers (*Pteruthius*) belong with New World Vireos (Vireonidae). Molecular Phylogenetics and Evolution 44:1352–1357.

Ree, R. H., and I. Sanmartín (2018). Conceptual and statistical problems with the DEC+J model of founder-event speciation and its comparison with DEC via model selection. Journal of Biogeography 45:741–749.

Remsen, J. V. Jr., J. I. Areta, C. D. Cadena, S. Claramunt, A. Jaramillo, J. F. Pacheco, M. B. Robbins, F. G. Stiles, D. F. Stotz, and K. J. Zimmer (2018). A classification of the bird species of South America. American Ornithological Society. https://www.museum.lsu.edu/~Remsen/SACCBaseline.htm.

Reid, N. (1991). Coevolution of mistletoes and frugivorous birds? Australian Journal of Ecology 16:457–469.

Ricklefs, R., and E. Bermingham (2008). The West Indies as a laboratory of biogeography and evolution. Philosophical Transactions of the Royal Society of London. Series B, Biological Sciences 363:2393–2413.

Salichos, L., A. Stamatakis, and A. Rokas (2014). Novel information theory-based measures for quantifying incongruence among phylogenetic trees. Molecular Biology and Evolution 31:1261–1271.

Simpson, G. G. (1980). Splendid Isolation: The Curious History of South American Mammals. Yale University Press, New Haven, CT, USA.

Smith, B. T., M. G. Harvey, B. C. Faircloth, T. C. Glenn, and R. T. Brumfield (2014). Target capture and massively parallel sequencing of ultraconserved elements for comparative studies at shallow evolutionary time scales. Systematic Biology 63:83–95.

Stamatakis, A. (2014). RAxML version 8: A tool for phylogenetic analysis and post-analysis of large phylogenies. Bioinformatics 30:1312–1313.

Tagliacollo, V. A., and R. Lanfear (2018). Estimating improved partitioning schemes for ultraconserved elements. Molecular Biology and Evolution 35:1798–1811.

Voelker, G. (1999). Dispersal, vicariance, and clocks: Historical biogeography and speciation in a cosmopolitan passerine genus (*Anthus*: Motacillidae). Evolution 53:1536–1552.

Voelker, G., S. Rohwer, D. C. Outlaw, and R. C. K. Bowie (2009). Repeated trans-Atlantic dispersal catalysed a global songbird radiation. Global Ecology and Biogeography 18:41–49.

Voelker, G., and G. M. Spellman (2004). Nuclear and mitochondrial DNA evidence of polyphyly in the avian superfamily Muscicapoidea. Molecular Phylogenetics and Evolution 30:386–394.

Walsberg, G. E. (1975). Digestive adaptations of *Phainopepla nitens* associated with the eating of mistletoe berries. The Condor 77:169–174.

Wetmore, A. (1914). The development of the stomach in the Euphonias. The Auk 31:458–461.

White, N. D., C. Mitter, and M. J. Braun (2017). Ultraconserved elements resolve the phylogeny of potoos (Aves: Nyctibiidae). Journal of Avian Biology 48:872–880.

Winker, K., T. C. Glenn, and B. C. Faircloth (2018). Ultraconserved elements (UCEs) illuminate the population genomics of a recent, high-latitude avian speciation event. PeerJ 2018:1–17.

Yang, Z., (1994). Estimating the pattern of nucleotide substitution. Journal of Molecular Evolution 39:105–111.

Younger, J. L., L. Strozier, J. D. Maddox, Á. S. Nyári, M. T. Bonfitto, M. J. Raherilalao, S. M. Goodman, and S. Reddy (2018). Hidden diversity of forest birds in Madagascar revealed using integrative taxonomy. Molecular Phylogenetics and Evolution 124:16–26.

Yuri, T., and D. P. Mindell (2002). Molecular phylogenetic analysis of Fringillidae, "New World nine-primaried oscines" (Aves: Passeriformes). Molecular Phylogenetics and Evolution 23:229–243.

Zhang, C., M. Rabiee, E. Sayyari, and S. Mirarab (2018). ASTRAL-III: Polynomial time species tree reconstruction from partially resolved gene trees. BMC Bioinformatics 19:153.

Zhang, S., L. Yang, X. Yang, and J. Yang (2007). Molecular phylogeny of the yuhinas (Sylviidae: *Yuhina*): A paraphyletic group of babblers including Zosterops and Philippine Stachyris. Journal of Ornithology 148:417–426.

Zuccon, D., R. Prys-Jones, D. P. C. Rasmussen, and P. G. P. Ericson (2012). The phylogenetic relationships and generic limits of finches (Fringillidae). Molecular Phylogenetics and Evolution 62:581–596.

APPENDIX TABLE 3. Read and UCE-matching contig data for individual specimens. Here, we specifically report the number of contigs that aligned with UCE loci in each assembly method and the mean length of those contigs

Taxon	Number of reads	# *Trinity* contigs	Mean contig length (bp)	# *SPAdes* contigs	Mean contig length (bp)
Fringilla montifringilla	2,124,977	3,896	550	–	–
Chlorophonia cyanea	2,863,854	4,312	833	4,312	837
Chlorophonia pyrrhophrys	142,039	3,779	396	3,776	393
Chlorophonia flavirostris	5,120,581	4,299	833	4,299	839
*Chlorophonia callophrys*_PA	6,248,855	4,347	847	4,374	852
*Chlorophonia callophrys*_CR	4,221,090	4,367	844	4,367	850
Euphonia jamaica	3,537,594	4,326	840	4,326	845
Euphonia plumbea	4,805,746	4,402	712	4,402	705
Euphonia affinis	4,417,426	4,350	844	4,350	849
Euphonia chlorotica	4,127,552	3,995	775	3,995	780
Euphonia luteicapilla	3,902,982	4,228	818	4,228	823
Euphonia trinitatis	3,359,767	4,231	646	4,231	639
Euphonia concinna	3,514,310	4,469	595	4,468	589
Euphonia saturata	6,142,221	4,328	841	4,327	846
Euphonia finschi	3,399,151	4,321	838	4,321	843
Euphonia violacea	5,393,351	4,300	831	4,300	834
Euphonia laniirostris	4,168,854	4,410	816	4,410	811
Euphonia hirundinacea	4,085,153	4,465	751	4,465	744
Euphonia chalybea	3,879,594	4,324	599	4,324	593
Euphonia musica	4,617,793	4,486	864	4,486	866
Euphonia elegantissima	3,557,976	4,367	713	4,367	706
Euphonia cyanocephala	6,501,897	4,289	831	4,289	837
Euphonia fulvicrissa	3,316,981	4,319	838	4,319	843
Euphonia chrysopasta	4,463,296	4,228	787	4,228	782
Euphonia mesochrysa	3,624,325	4,443	790	4,443	783
Euphonia imitans	2,662,905	4,373	845	4,373	850
Euphonia gouldi	4,492,017	4,485	869	4,485	874
Euphonia minuta	3,521,382	4,285	830	4,285	834
Euphonia anneae	1,160,476	4,231	673	4,230	666
Euphonia xanthogaster quitensis	5,197,535	4,331	839	4,331	845
Euphonia xanthogaster ruficeps	3,565,327	4,235	821	4,235	826
Euphonia cayennensis	830,473	4,286	809	4,282	809
Euphonia pectoralis	4,266,659	4,399	852	4,398	857
Euphonia rufiventris	4,384,654	4,181	812	4,181	817
Coccothraustes vespertinus	3,332,298	4,295	828	4,292	833
Spinus tristis	4,056,414	4,266	823	4,264	827
Emberiza cintrinella	4,941,509	4,035	636	–	–

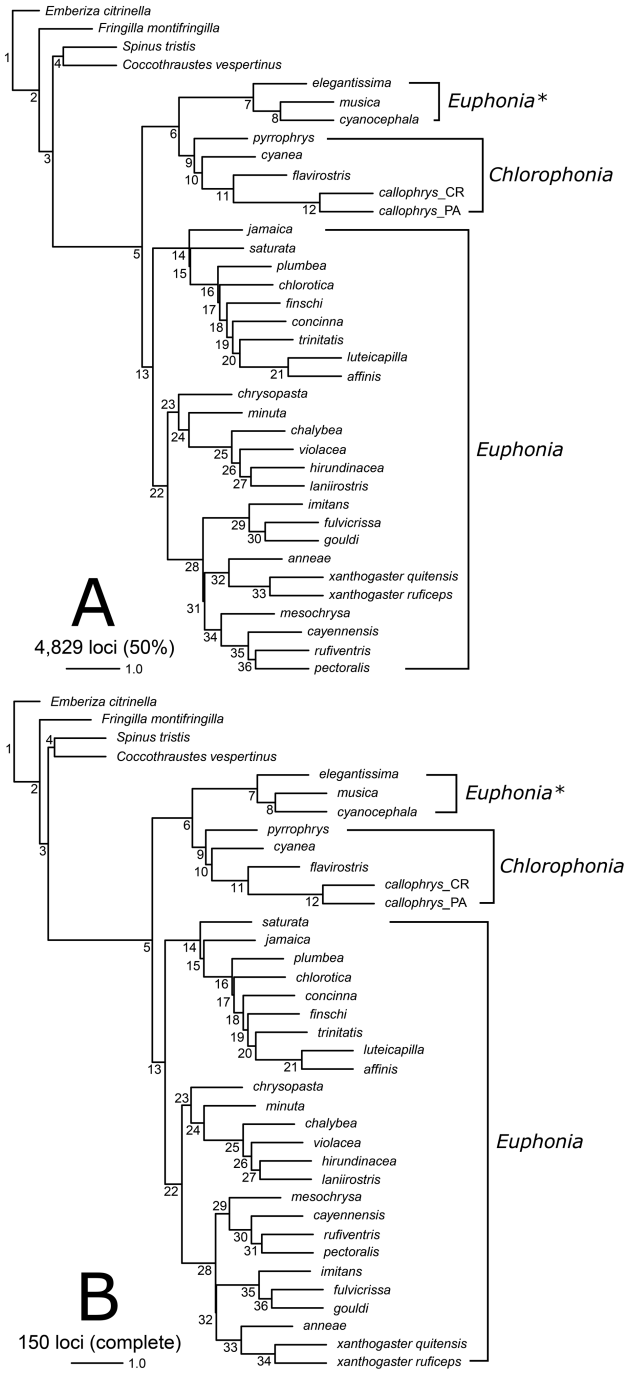

APPENDIX FIGURE 5. ASTRAL species trees generated from rarified UCE datasets. The top tree (**A**) was inferred from an ASTRAL analysis including 4,829 loci, for which ≥ 50% of species were sampled, and the bottom tree (**B**) was inferred from a separate analysis including only the 150 loci that were found in all species in this study. The *Euphonia* clade marked with an asterisk designates the blue-hooded species.

APPENDIX TABLE 4. Node support values and node ages from the total ASTRAL species tree topology inferred for this study. These node values correspond to the total ASTRAL species tree that was made ultrametric in BEAST2 in Appendix Figure 6. The first 2 nodes lack these support values as a result of rooting the tree with the appropriate outgroups, but we do report ages inferred for these nodes in BEAST2

Node	LPP	gCF	sCF	IC	Bootstrap	Age (Myr)	Age (95% HPD)
1	–	–	–	–	–	16.80	14.50–19.25
2	–	–	–	–	–	14.60	12.35–16.51
3	1	39.8	51.1	0.020	100	13.80	11.83–15.77
4	1	77.2	89.0	0.614	100	7.06	5.97–8.02
5	1	19.5	47.2	0.136	100	6.49	5.42–7.29
6	1	18.1	50.6	0.204	100	5.68	4.84–6.49
7	1	30.8	70.2	0.377	100	4.25	3.63–4.86
8	1	10.9	35.0	0.000	100	3.96	3.43–4.60
9	1	27.2	58.9	0.278	100	3.24	2.74–3.70
10	1	38.8	70.8	0.353	100	2.35	1.97–2.70
11	1	29.5	41.7	0.025	100	1.85	1.51–2.11
12	1	36.8	70.5	0.392	100	2.67	2.21–3.06
13	1	57.6	73.9	0.358	100	1.32	1.12–1.56
14	1	48.8	79.5	0.634	100	2.54	2.11–2.90
15	1	42.5	59.0	0.114	100	1.89	1.57–2.17
16	1	18.5	47.7	0.093	100	5.17	4.35–5.85
17	1	23.7	50.0	0.116	100	4.58	3.88–5.24
18	1	52.6	86.4	0.510	100	2.58	2.18–2.99
19	1	27.7	47.7	0.054	100	2.34	1.96–2.69
20	1	28.8	50.1	0.041	100	2.01	1.68–2.32
21	1	34.9	70.0	0.322	100	4.80	4.07–5.46
22	0.76	14.9	34.3	0.009	87	4.44	3.82–5.12
23	1	30.3	71.1	0.251	100	3.43	2.93–3.96
24	0.98	10.4	33.9	0.000	90	3.16	2.68–3.61
25	1	16.1	48.3	0.066	100	2.44	2.07–2.81
26	1	17.7	49.7	0.044	100	2.14	1.81–2.48
27	1	21.8	49.1	0.028	100	1.81	1.54–2.13
28	1	58.7	81.7	0.526	100	0.68	0.56–0.82
29	1	38.7	69.8	0.360	100	5.14	4.40–5.89
30	1	34.2	77.9	0.091	100	3.84	3.28–4.41
31	1	24.3	20.8	0.025	100	3.72	3.13–4.23
32	1	46.4	74.0	0.180	100	2.65	2.27–3.10
33	–	–	–	–	–	1.97	1.52–2.37
34	1	79.1	96.3	0.643	100	0.55	0.44–0.67
35	1	72.9	93.1	0.584	100	1.96	1.63–2.27
36	1	54.4	69.8	0.157	100	1.40	1.18–1.64
37	1	35.8	43.2	0.008	100	13.04	11.12–14.84

APPENDIX TABLE 5. Node support values for rarified ASTRAL species trees. The corresponding ASTRAL species trees inferred from the 50% complete and complete sequence matrices are in Appendix Figure 5. The left set of columns contain node support values for the 50% complete tree, and the right set those of the complete tree

Node	50% (4,829 loci)				Complete (150 loci)			
	LPP	gCF	sCF	IC	LPP	gCF	sCF	IC
1	–	–	–	–	–	–	–	–
2	–	–	–	–	–	–	–	–
3	1	39.7	51.1	-0.001	0.99	33.3	50.4	0.040
4	1	35.8	43.2	0.006	0.92	30.0	42.0	0.025
5	1	77.3	89.0	0.334	1	82.0	91.3	0.882
6	1	38.6	69.6	0.117	1	40.7	72.4	0.522
7	1	72.9	93.1	0.573	1	70.0	94.6	0.773
8	1	54.3	69.8	0.130	1	47.3	66.6	0.099
9	1	34.1	76.9	0.061	1	32.7	78.6	0.107
10	1	24.3	20.9	0.012	0.93	19.3	25.6	0.002
11	1	46.4	74.3	0.112	1	46.7	80.5	0.252
12	1	79.1	96.4	0.557	1	76.7	96.7	0.653
13	1	19.5	47.3	0.110	1	20.0	45.9	0.137
14	1	34.9	70.4	0.270	1	38.7	73.3	0.600
15	0.72	14.9	34.2	0.001	0.59	17.3	37.4	0.000
16	1	30.3	70.7	0.153	1	30.0	74.7	0.350
17	0.98	10.4	34.1	0.002	0.54	8.7	35.8	-0.040
18	1	16.1	48.4	0.050	0.99	20.0	65.6	0.056
19	1	17.7	49.8	0.058	0.57	6.7	23.1	-0.104
20	1	21.8	49.1	0.032	0.96	16.7	60.4	0.013
21	1	58.7	81.8	0.468	1	61.3	86.1	0.437
22	1	18.1	50.4	0.142	1	23.3	55.4	0.523
23	1	18.6	47.4	0.081	0.99	14.0	46.7	0.093
24	1	23.7	50.3	0.074	1	24.7	54.9	0.101
25	1	52.5	86.1	0.487	1	55.3	90.1	0.571
26	1	27.7	47.6	0.028	0.98	28.0	43.7	0.024
27	1	28.8	50.0	0.045	0.98	26.7	42.7	0.027
28	1	30.8	70.4	0.165	1	32.7	75.3	0.555
29	1	48.7	79.7	0.375	1	26.0	59.3	0.342
30	1	42.5	59.7	0.117	1	29.3	69.1	0.278
31	0.99	10.8	35.0	0.000	1	28.0	55.6	0.054
32	1	36.9	70.4	0.254	0.42	10.0	34.0	0.000
33	1	57.6	73.8	0.329	1	33.3	69.4	0.421
34	1	27.2	58.5	0.228	1	51.3	74.9	0.266
35	1	38.8	71.1	0.253	1	48.0	86.3	0.609
36	1	29.5	41.7	0.020	1	40.0	60.8	0.082

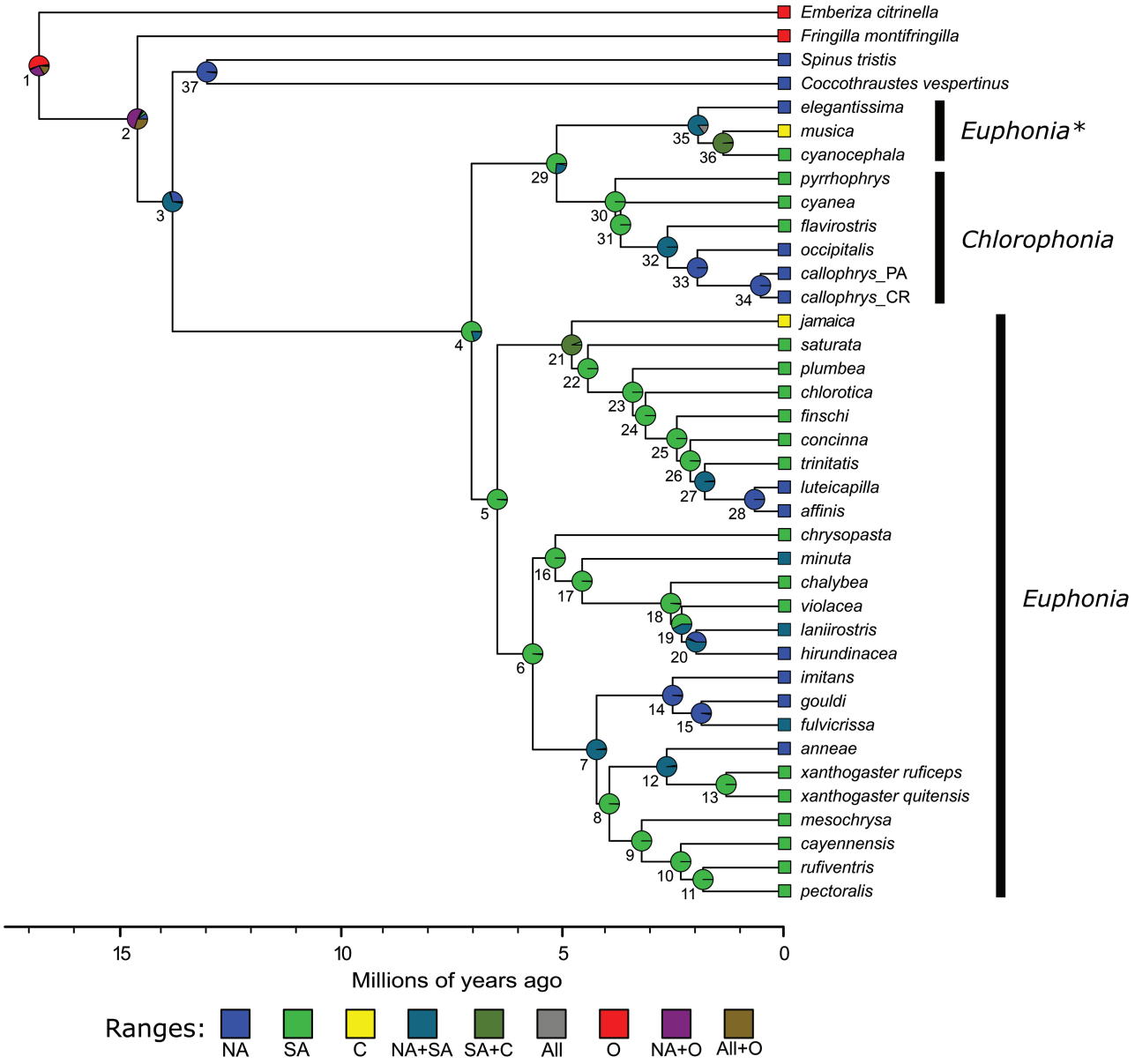

APPENDIX FIGURE 6. Biogeographic history and Bayesian time-scaled phylogeny of Euphoniinae and outgroups. Node numbers correspond to the values of node support in Appendix Table 4, and the pie charts at each node show the proportional likelihood of possible ancestral ranges inferred by the DIVALIKE model. An additional area O (Eastern Hemisphere) was included in the total analysis for the Eurasian outgroup species, *Fringilla montifringilla* and *Emberiza citrinella*.

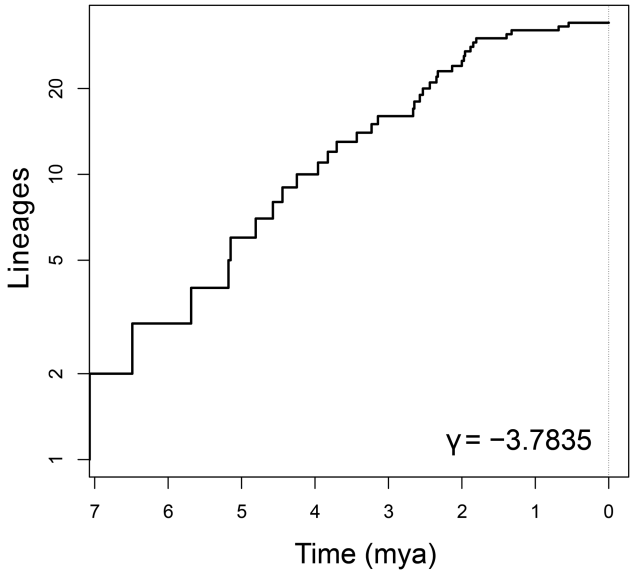

APPENDIX FIGURE 7. Lineages-through-time plot from the Euphoniinae subtree. The γ-statistic was calculated using the *ltt* function in the R package *phytools* and was highly significant ($P < 0.001$).